JP0250379

JAERI-Data/Code
2002-015

DATA ON LOSS OF OFF-SITE ELECTRIC POWER SIMULATION TESTS OF THE HIGH TEMPERATURE ENGINEERING TEST REACTOR

July 2002

Takeshi TAKEDA, Shigeaki NAKAGAWA, Nozomu FUJIMOTO
Yukio TACHIBANA and Tatsuo IYOKU

日本原子力研究所
Japan Atomic Energy Research Institute

本レポートは，日本原子力研究所が不定期に公刊している研究報告書です。
入手の問合わせは，日本原子力研究所研究情報部研究情報課（〒319-1195　茨城県那珂郡東海村）あて，お申し越しください。なお，このほかに財団法人原子力弘済会資料センター（〒319-1195　茨城県那珂郡東海村日本原子力研究所内）で複写による実費頒布をおこなっております。

This report is issued irregularly.
Inquiries about availability of the reports should be addressed to Research Information Division, Department of Intellectual Resources, Japan Atomic Energy Research Institute, Tokai-mura, Naka-gun, Ibaraki-ken, 319-1195, Japan.

編集兼発行　　日本原子力研究所

JAERI-Data/Code 2002-015

Data on Loss of Off-site Electric Power Simulation Tests of the High Temperature Engineering Test Reactor

Takeshi TAKEDA, Shigeaki NAKAGAWA, Nozomu FUJIMOTO,
Yukio TACHIBANA and Tatsuo IYOKU

Department of HTTR Project
Oarai Research Establishment
Japan Atomic Energy Research Institute
Oarai-machi, Higashiibaraki-gun, Ibaraki-ken

(Received June 4, 2002)

The high temperature engineering test reactor (HTTR), the first high temperature gas-cooled reactor (HTGR) in Japan, achieved the first full power of 30 MW on December 7 in 2001. In the rise-to-power test of the HTTR, simulation tests on loss of off-site electric power from 15 and 30 MW operations were carried out by manual shutdown of off-site electric power. Because helium circulators and water pumps coasted down immediately after the loss of off-site electric power, flow rates of helium and water decreased to the scram points. To shut down the reactor safely, the subcriticality should be kept by the insertion of control rods and the auxiliary cooling system should cool the core continuously avoiding excessive cold shock to core graphite components. About 50 s later from the loss of off-site electric power, the auxiliary cooling system started up by supplying electricity from emergency power feeders. Temperature of hot plenum block among core graphite structures decreased continuously after the startup of the auxiliary cooling system. This report describes sequences of dynamic components and transient behaviors of the reactor and its cooling system during the simulation tests from 15 and 30 MW operations.

Keywords: HTGR, HTTR, Rise-to-power Test, Loss of Off-site Electric Power, Simulation, Evaluation, Experiment, Reactor Scram, Transient Behavior, Auxiliary Cooling System

JAERI-Data/Code 2002-015

高温工学試験研究炉の商用電源喪失模擬試験データ

日本原子力研究所大洗研究所高温工学試験研究炉開発部
竹田 武司・中川 繁昭・藤本 望・橘 幸男・伊与久 達夫

(2002年6月4日受理)

ＨＴＴＲ(高温工学試験研究炉)は日本で初めての高温ガス炉(ＨＴＧＲ)であり,2001年12月7日に初めて全出力(30MW)を達成した。ＨＴＴＲの出力上昇試験の中で,15MW,30MW 運転から商用電源の手動遮断により商用電源喪失模擬試験を実施した。商用電源喪失直後,ヘリウム循環機および加圧水ポンプはコーストダウンし,ヘリウムおよび加圧水の流量はスクラム設定値まで減少した。原子炉を安全に停止するためには,制御棒の挿入により未臨界状態を維持するとともに炉心黒鉛構造物の過度なコールドショックを防止しながら,補助冷却設備により炉心を継続的に冷却する。商用電源喪失から約50 秒後,非常用発電機からの給電により補助冷却設備は起動した。補助冷却設備の起動後,炉内黒鉛構造物である高温プレナムブロックの温度は継続的に低下した。本報は,15MW, 30MW 運転からの商用電源喪失模擬試験時の動的機器のシーケンス,原子炉および原子炉冷却設備の過渡挙動について報告するものである。

大洗研究所：〒311-1394 茨城県東茨城郡大洗町成田町新堀 3607

Contents

1. Introduction ····· 1
2. Outline of Core Components, Reactor Internals and Auxiliary Cooling System ····· 9
3. Sequences of Dynamic Components during Simulation Tests ····· 15
4. Behaviors of Reactor and its Cooling System at Simulation Tests ····· 23
4.1 Conditions of Reactor and its Cooling System before Simulation Tests ····· 23
4.2 Transient Behaviors of Reactor and its Cooling System during Simulation Tests ···25
5. Conclusions ····· 38
Acknowledgements ····· 39
References ····· 39

目　次

1．緒　言 ····· 1
2．炉心構成要素，炉内構造物および補助冷却設備の概要 ····· 9
3．模擬試験時の動的機器のシーケンス ····· 15
4．模擬試験における原子炉および原子炉冷却設備の挙動 ····· 23
4．1　模擬試験前の原子炉および原子炉冷却設備の条件 ····· 23
4．2　模擬試験時の原子炉および原子炉冷却設備の過渡挙動 ····· 25
5．結　言 ····· 38
謝　辞 ····· 39
参考文献 ····· 39

This is a blank page.

List of Tables

Table 1.1 Major specifications of the HTTR

Table 4.1 Conditions of reactor before simulation tests

Table 4.2 Conditions of intermediate heat exchanger before simulation tests

Table 4.3 Conditions of primary pressurized water cooler before simulation tests

Table 4.4 Conditions of secondary pressurized water cooler before simulation tests

Table 4.5 Conditions of air cooler for pressurized water cooling system before simulation tests

Table 4.6 Conditions of auxiliary heat exchanger before simulation tests

Table 4.7 Conditions of air cooler for auxiliary cooling system before simulation tests

Table 4.8 Pressure ratio of outlet to inlet and invariant power of primary and secondary helium circulators before simulation tests

Table 4.9 Typical pressure ratio of outlet to inlet of auxiliary helium circulators during simulation tests

List of Figures

Fig. 1.1 Bird's-eye view of reactor pressure vessel and core

Fig. 1.2 Horizontal cross section of reactor core

Fig. 1.3 Schematic diagram of reactor cooling system

Fig. 1.4 Configuration of fuel assembly

Fig. 1.5 Bird's-eye view of control rod system

Fig. 2.1 Bird's-eye view of reactor internals

Fig. 2.2 Bird's-eye view of auxiliary heat exchanger

Fig. 2.3 Cross-sectional view of auxiliary concentric hot gas duct

Fig. 2.4 Bird's-eye view of auxiliary helium circulator

Fig. 2.5 Structural drawing of air cooler for auxiliary cooling system

Fig. 3.1 Sequence of dynamic components during loss of off-site electric power simulation test from 15 MW operation

Fig. 3.2 Sequence of dynamic components during loss of off-site electric power simulation test from 30 MW operation

Fig. 3.3 Transient behaviors of rotations of all primary and secondary helium circulators during loss of off-site electric power simulation test from 15 MW operation

Fig. 3.4 Transient behaviors of rotations of all primary and secondary helium circulators during loss of off-site electric power simulation test from 30 MW operation

Fig. 3.5 Transient behaviors of rotation and flow rate of auxiliary helium circulators during loss of off-site electric power simulation test from 15 MW operation

Fig. 3.6 Transient behaviors of rotation and flow rate of auxiliary helium circulators during loss of off-site electric power simulation test from 30 MW operation

Fig. 4.1 Cross-sectional view of graphite blocks just below active reactor core

Fig. 4.2 Design performance curve of helium circulators for primary and secondary helium cooling systems

Fig. 4.3 Design performance curve of helium circulators for auxiliary cooling system

Fig. 4.4 Transient behaviors of temperatures of hot plenum block, reactor inlet and outlet coolant during loss of off-site electric power simulation test from 15 MW operation

Fig. 4.5 Transient behaviors of temperatures of hot plenum block, reactor inlet and outlet coolant during loss of off-site electric power simulation test from 30 MW operation

Fig. 4.6 Transient behaviors of primary coolant pressure and reactor power during loss of off-site electric power simulation test from 15 MW operation

Fig. 4.7 Transient behaviors of primary coolant pressure and reactor power during loss of off-site electric power simulation test from 30 MW operation

Fig. 4.8 Transient behavior of heat removal of auxiliary heat exchanger during loss of off-site electric power simulation test from 15 MW operation

Fig. 4.9 Transient behavior of heat removal of auxiliary heat exchanger during loss of off-site electric power simulation test from 30 MW operation

1. Introduction

The high temperature gas-cooled reactor (HTGR) is expected very much as one of the advanced nuclear reactors in the future because it can supply high temperature heat and thus produce electricity with high thermal efficiency. The HTGR also has inherent safety characteristics by its large heat capacity and low power density of the core compared with conventional light water reactors. Accordingly, the temperature change of the HTGR core is extremely small for the transient variation of the reactor power and for the excessive performance deterioration of the reactor cooling system. Japan Atomic Energy Research Institute (JAERI) built a graphite-moderated and helium-gas-cooled reactor, the high temperature engineering test reactor (HTTR) [1]. Figures 1.1 and 1.2 show a bird's-eye view of the reactor pressure vessel and core and the horizontal cross section of the reactor core, respectively. The major specifications of the HTTR are summarized in Table 1.1. The HTTR is the first HTGR in Japan with reactor outlet coolant gas temperature of 850°C at rated operation and 950°C at high temperature test operation with thermal power of 30 MW, using pin-in-block type fuel.

Figure 1.3 shows a schematic diagram of the reactor cooling system of the HTTR. The reactor cooling system consists of the main cooling system, the auxiliary cooling system [2] and the vessel cooling system [3]. The main cooling system consists of the primary and secondary helium cooling systems as well as the pressurized water cooling system. The auxiliary cooling system is in standby during the reactor normal operation, and starts up automatically to cool the core directly when the reactor scrams in an accident when forced circulation can cool the core. To shut down the reactor safely, the subcriticality should be kept by the insertion of control rods and the auxiliary cooling system should cool the core continuously avoiding excessive cold shock to core graphite components such as fuel elements (Fig. 1.4). The auxiliary cooling system is mainly composed of a heat exchanger, helium circulators, concentric hot gas duct, water pumps and air cooler. The vessel cooling system works to cool the biological concrete shield during the normal operation and is employed to remove decay heat and residual heat in an accident when forced

circulation cannot cool the core.

Figure 1.5 shows a bird's-eye view of the control rod system of the HTTR. The electromagnetic clutch is separated to insert control rods into the reactor core by gravity when electric current through the clutch is cut off by a reactor scram signal. The clad material of the control rod is ferritic superalloy Alloy 800H. The maximum allowable temperature for the control rod to be used repeatedly after scrams is 900°C [4]. Accordingly, in reactor scram cases from operation of the reactor outlet coolant temperature of more than 750°C except a depressurized accident [3], the control rods are inserted at the two-steps for preventing the control rod clad from overcooling.

The rise-to-power test of the HTTR started on September 28 in 1999. JAERI planned to carry out simulation tests on loss of off-site electric power from 15 and 30 MW in the rise-to-power test. The thermal power rose up to 20 MW at rated operation in February 2001. The HTTR attained its first full power of 30 MW at rated operation on December 7 in 2001. The simulation test from 15 MW operation (effective full power days: about 20 days) was conducted on March 1 in 2001. On the contrary, the simulation test from 30 MW operation (effective full power days: about 120 days) was performed on March 6 in 2002.

In this report, sequences of dynamic components (e.g., main helium circulators) and transient behaviors of the reactor and its cooling system during the simulation tests from 15 and 30 MW operations are presented. The outline of the major components and system, other thermal and nuclear data set are described in published report (5) by JAERI.

Table 1.1 Major specifications of the HTTR

Thermal power	30 MW
Outlet coolant temperature	850°C (rated operation), 950°C (high temperature test operation)
Inlet coolant temperature	395°C
Flow rate of primary coolant	12.4 kg/s (rated operation), 10.2 kg/s (high temperature test operation)
Primary coolant pressure	4 MPa
Core structure	Graphite
Equivalent core diameter	2.3 m
Effective core height	2.9 m
Average power density	2.5 W/cm^3
Fuel	Low-enriched UO_2
Uranium enrichment	3-10 wt% (average 6 wt%)
Fuel type	Pin-in-block
Coolant	Helium gas
Direction of coolant flow	Downward flow
Number of fuel assembly	150
Number of fuel columns	30
Plant lifetime	20 years

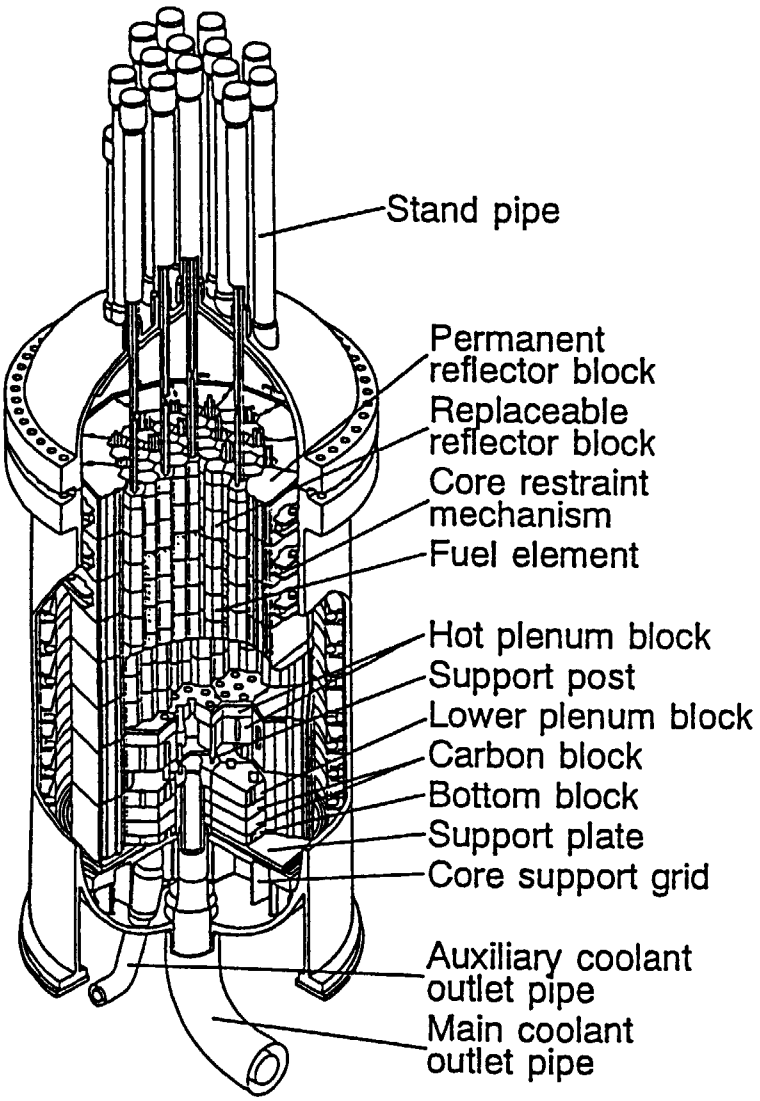

Fig. 1.1 Bird's-eye view of reactor pressure vessel and core

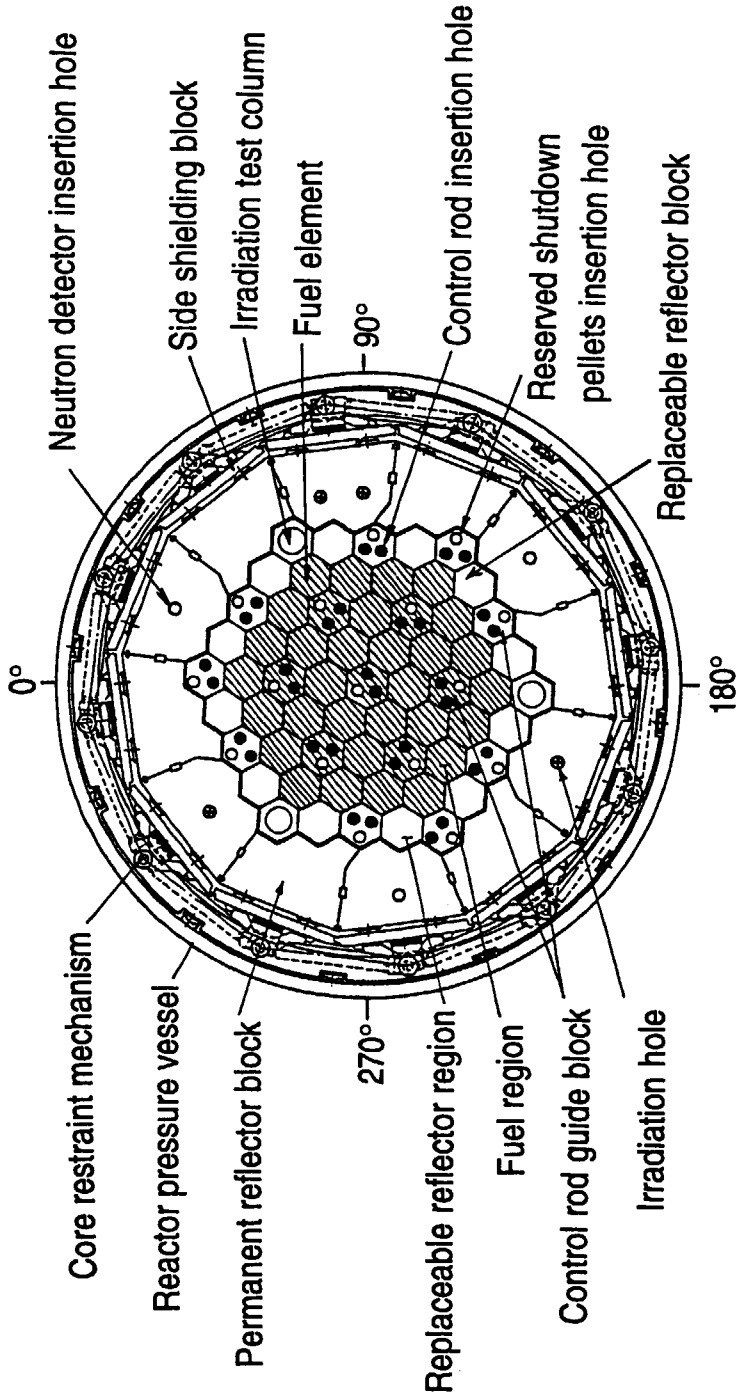

Fig. 1.2 Horizontal cross section of reactor core

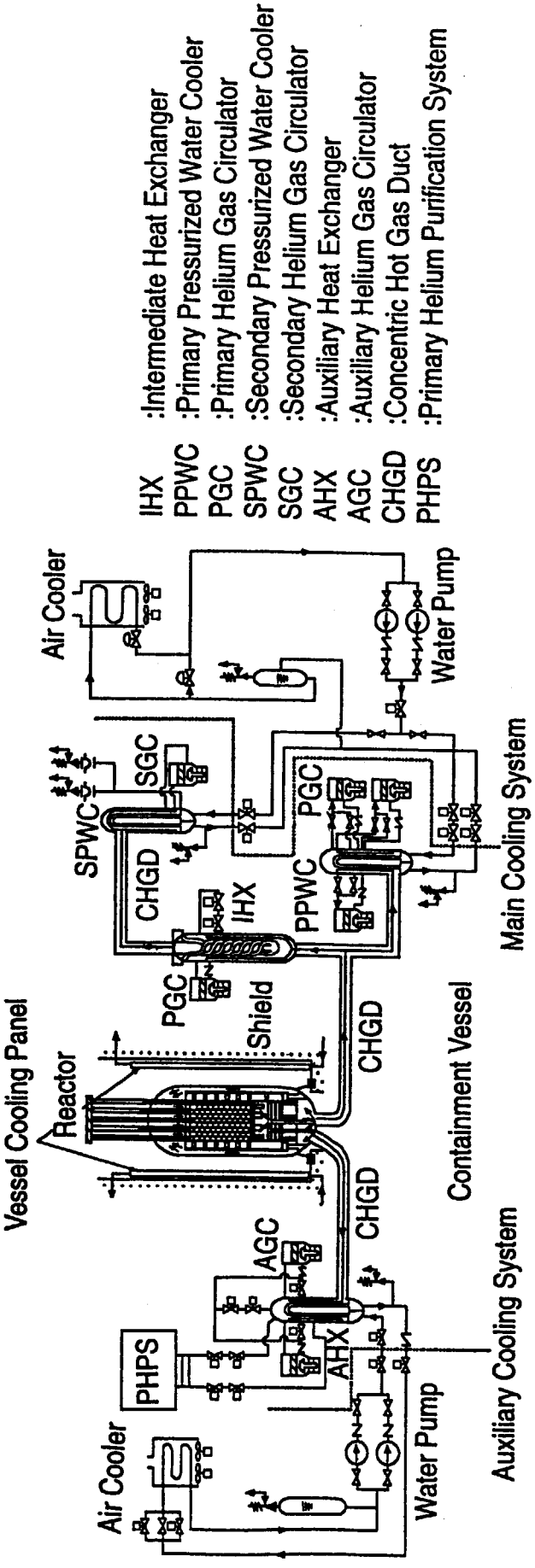

Fig. 1.3 Schematic diagram of reactor cooling system

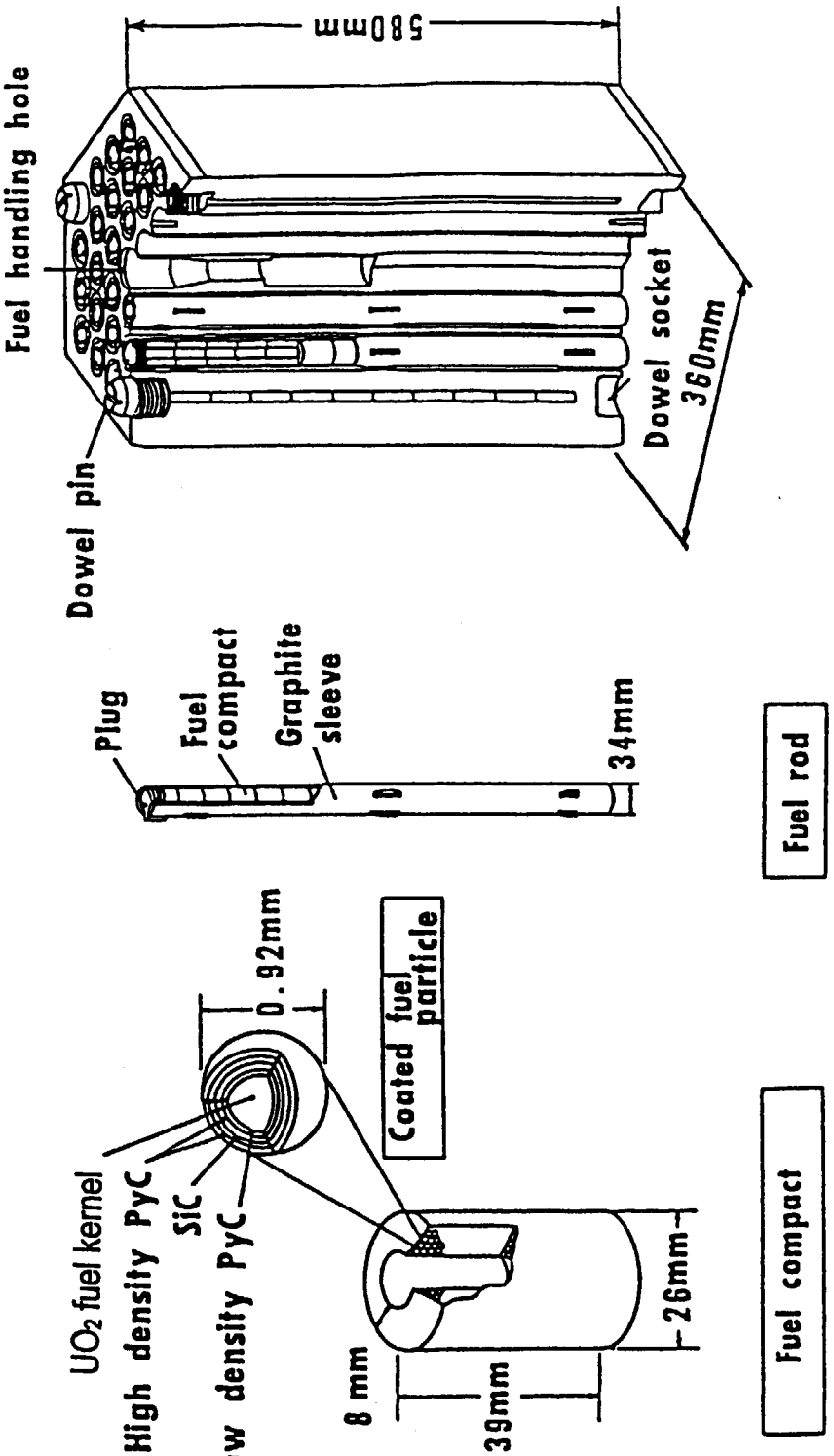

Fig. 1.4 Configuration of fuel assembly

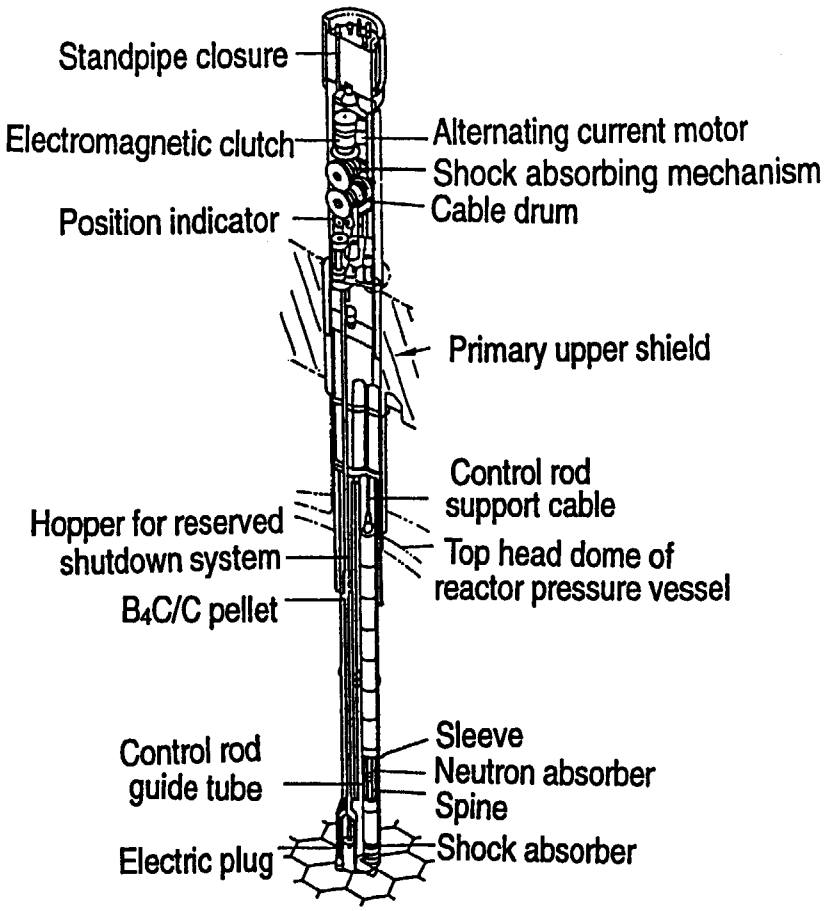

Fig. 1.5 Bird's-eye view of control rod system

2. Outline of Core Components, Reactor Internals and Auxiliary Cooling System

The reactor consists of core components, reactor internals, reactor pressure vessel and so on. As shown in Fig. 1.4, the prismatic hexagonal fuel graphite block is 580 mm in height and 360 mm in width across the flats. Tri-isotropic coated fuel particles with low-enriched UO_2 kernel of 6 wt % in average enrichment are dispersed in the graphite matrix. The active reactor core, 2.9 m in height and 2.3 m in effective diameter, consists of 30 fuel columns and seven control rod graphite block columns, each column being composed of five blocks. Helium flows downward through each annular gap between the vertical hole in the hexagonal graphite block and the fuel rod to remove heat by fission and gamma heating. The reactor internals are composed of graphite and metallic core support structures as well as shielding blocks as shown in Fig. 2.1. The graphite core support structures contain hot plenum blocks, permanent reflector blocks, support posts and core bottom structures.

As shown in Fig. 2.2, the auxiliary heat exchanger is a vertical inverse-U-tube type heat exchanger, similar to the primary and secondary pressurized water coolers. Helium flows on the shell side, while pressurized water goes into the heat transfer tubes. Hot helium is transported from the reactor core to the auxiliary heat exchanger through the auxiliary concentric hot gas duct (Fig. 2.3). Hot helium from the inlet nozzle flows horizontally between the baffle plates, and cools the outer surface of the heat transfer tubes. Hot helium once goes out to the auxiliary helium circulators (Fig. 2.4), and goes back to the annular path between the inner and outer shells. Pressurized water from the inlet nozzle flows into the water chamber, and goes upward in the heat transfer tubes. As shown in Fig. 2.5, air flowing on the shell side through four motor-driven fans of the air cooler for the auxiliary cooling system cools the outer surface of the heat transfer tubes. Decay heat of fission products and residual heat of the reactor core are finally dissipated to the heat sink of atmosphere by the air cooler for the auxiliary cooling system.

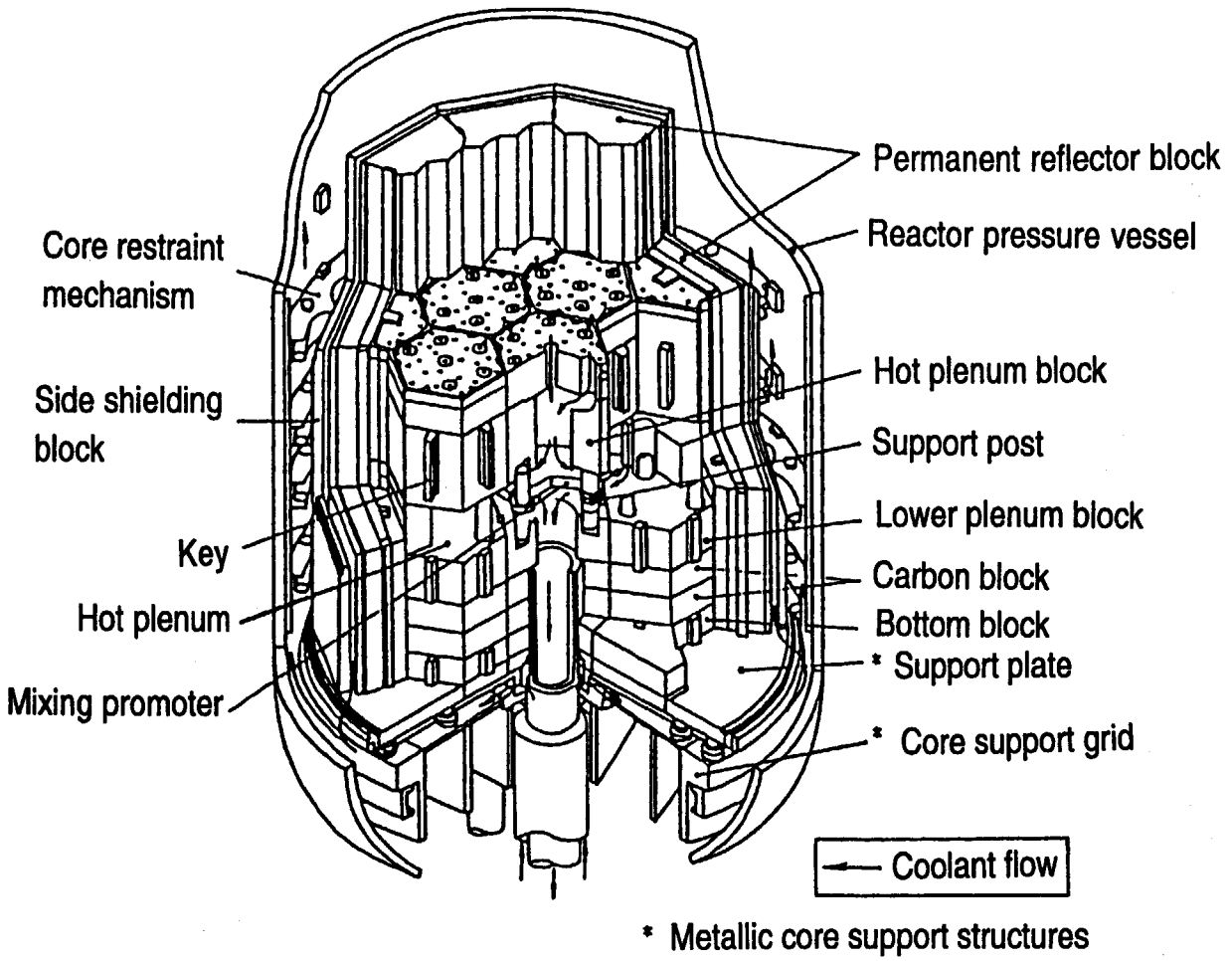

Fig. 2.1 Bird's-eye view of reactor internals

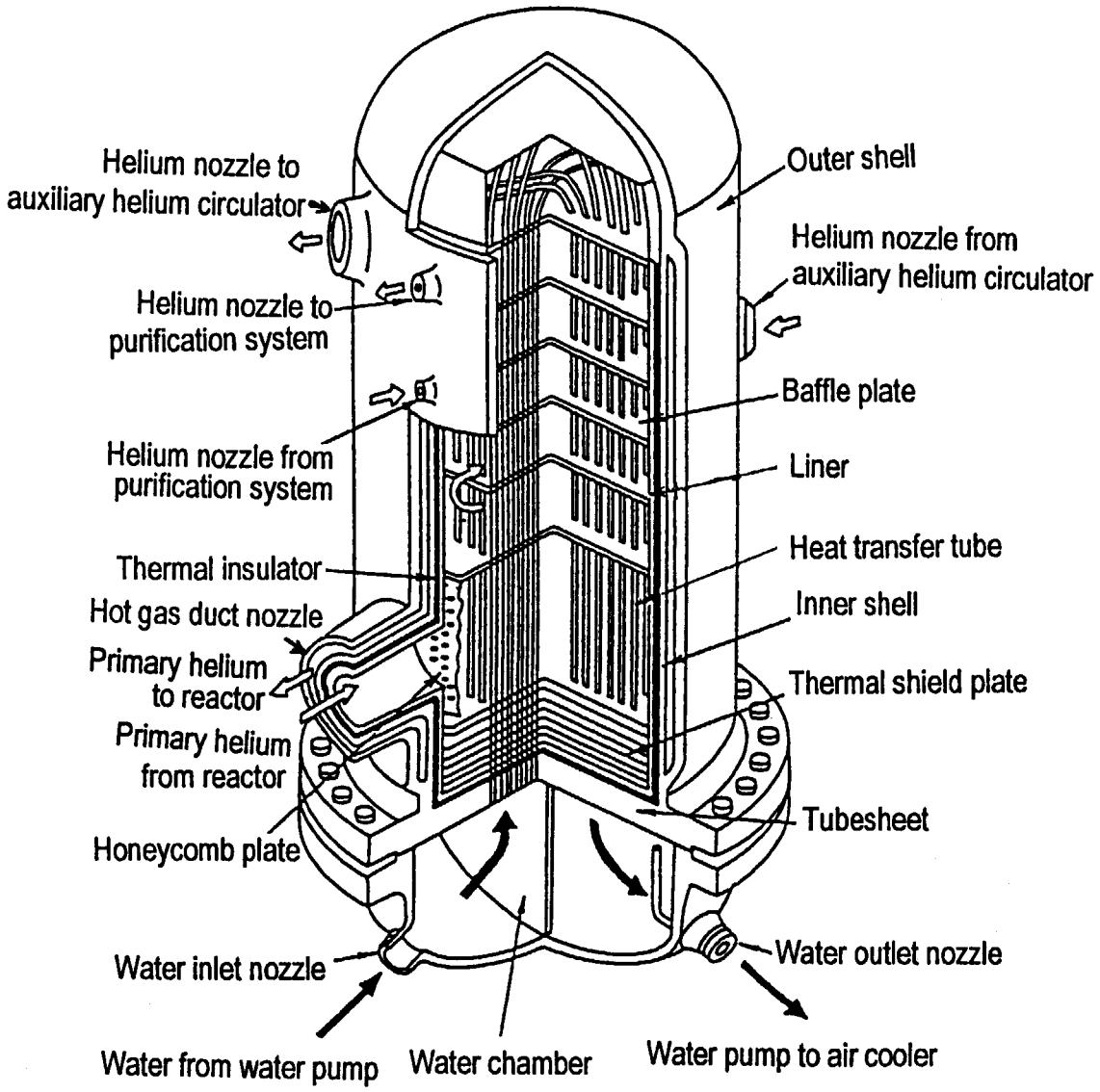

Fig. 2.2 Bird's-eye view of auxiliary heat exchanger

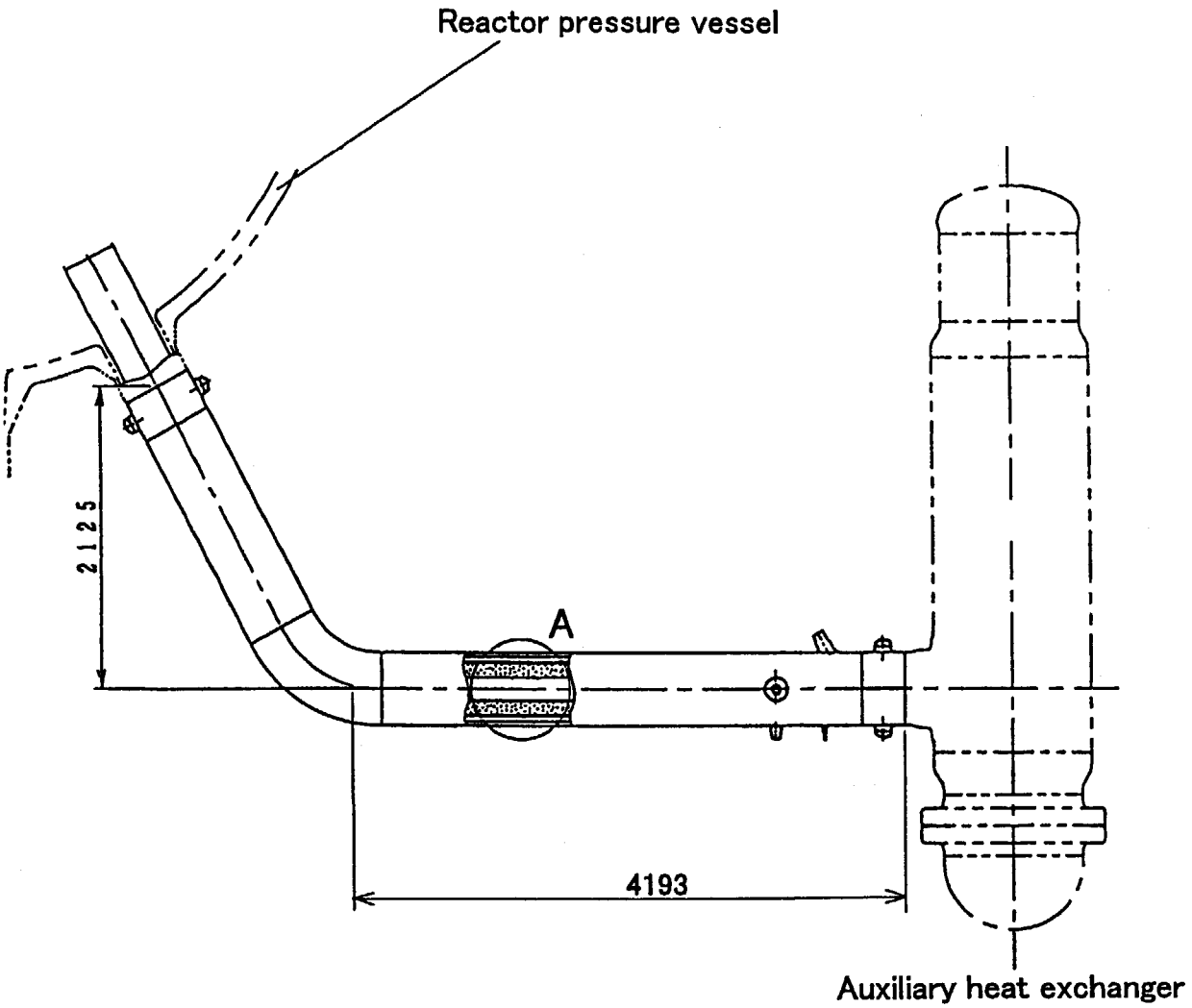

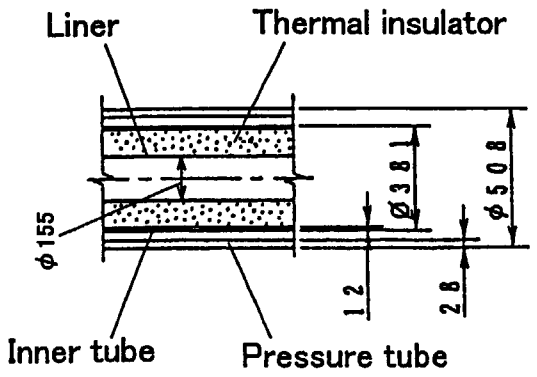

A in detail

Fig. 2.3 Cross-sectional view of auxiliary concentric hot gas duct

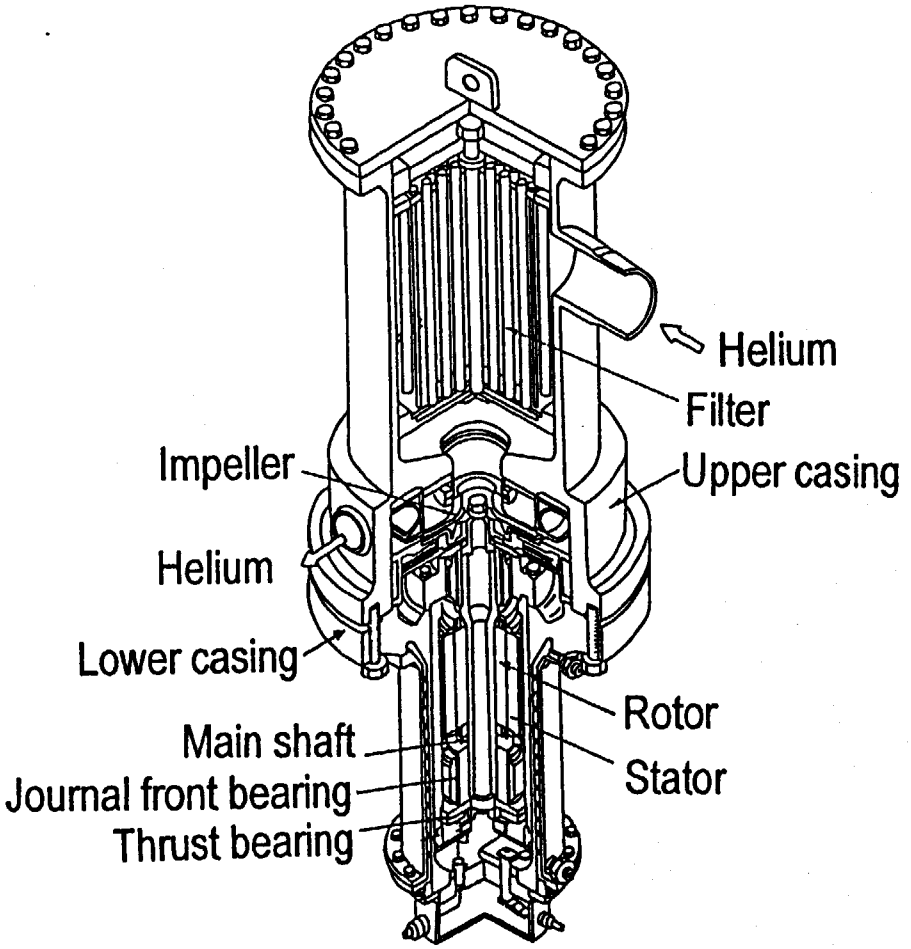

Fig. 2.4 Bird's-eye view of auxiliary helium circulator

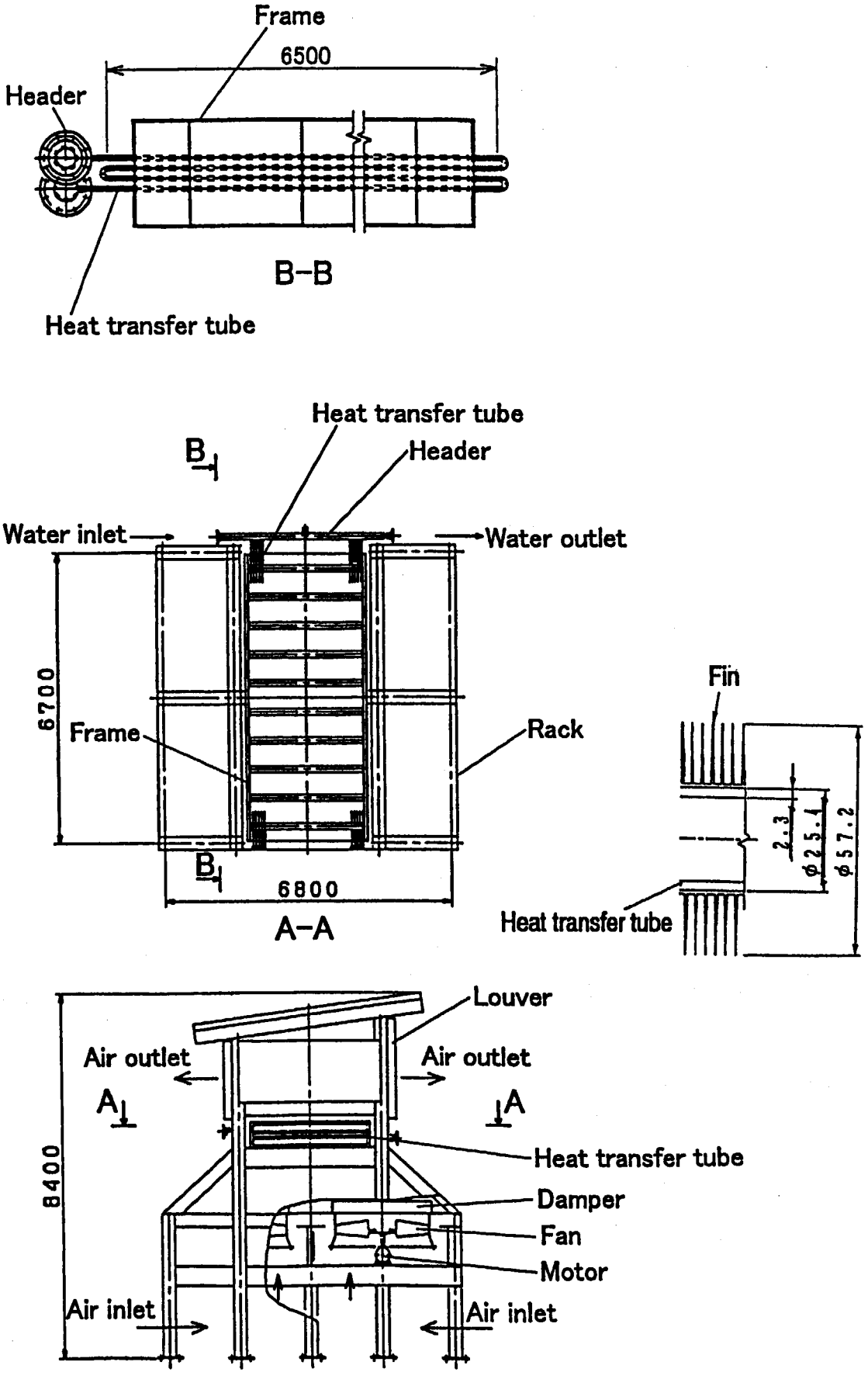

Fig. 2.5 Structural drawing of air cooler for auxiliary cooling system

3. Sequences of Dynamic Components during Simulation Tests

Figures 3.1 and 3.2 show sequences of the dynamic components during the simulation tests from 15 and 30 MW operations, respectively. Although the loss of off-site electric power is caused by failure of the power transmission line or the HTTR electrical equipment, the simulation tests were carried out by manual shutdown of off-site electric power of the HTTR. All the primary and secondary helium circulators as well as the water pumps for the pressurized water, the auxiliary and the vessel cooling systems coasted down immediately after the loss of off-site electric power. Accordingly, flow rates of primary and secondary helium as well as water reduced. 1.6 s later from the loss of off-site electric power, the reactor scrammed by the reactor protection system, in other words, the reactor scram breaker was open.

At the simulation test from 15 MW operation, the reactor scram occurred by decreasing flow rate of primary helium of the intermediate heat exchanger to the scram point of 3.8 kg/s (92 % of the total). At the simulation test from 30 MW operation, the reactor scram happened by decreasing flow rate of helium of the primary pressurized water cooler to the scram point of 7.7 kg/s (93 % of the total).

At the simulation test from 15 MW operation, all the control rods were inserted simultaneously into the reactor core by gravity within the design criterion of 12 s because the helium inlet temperature of the auxiliary heat exchanger was below 750°C. At the simulation test from 30 MW operation, the outer nine pairs of the control rods were inserted into the replaceable reflector region of the core within 12 s at first because the helium inlet temperature of the auxiliary heat exchanger was 750°C, and 40 min later the other inner seven pairs fell into the fuel region within 12 s.

About 2 s later from the reactor scram, braking of all the primary and secondary helium circulators was initiated by flowing electric current from their associated batteries. Figures 3.3 and 3.4 show transient behaviors of the rotations of all the primary and secondary helium circulators during the simulation tests from 15 and 30 MW operations, respectively.

Although all the helium circulators for the primary pressurized water cooler are the same dimensions, each of the helium circulators has its own characteristics of rotation, flow rate and pressure rise. The braking stop times, when the rotations of the helium circulators became to zero, were 10 s or less after the open of the reactor scram breaker.

About 50 s later from the loss of off-site electric power, the auxiliary cooling system and the vessel cooling system started up by supplying electricity from two emergency power feeders. Figures 3.5 and 3.6 show transient behaviors of the rotation and the flow rate of the auxiliary helium circulators during the simulation tests from 15 and 30 MW operations, respectively. About 1 s later from the startup of the auxiliary cooling system, the rotations of the two auxiliary helium circulators reached about 3000 min^{-1}. This rotation was kept for about 2 s. After that, the rotations of the two auxiliary helium circulators rose up to about 8500 min^{-1} at the constant rate by the automatic frequency control. About 14 s later from the startup of the auxiliary cooling system, helium flow rates of the auxiliary helium circulators (A) and (B) reached about 0.73 kg/s and about 0.75 kg/s respectively at the simulation test from 15 MW operation, while they achieved about 0.85 kg/s and about 0.89 kg/s at the simulation test from 30 MW operation.

40 min later from the startup of the auxiliary cooling system, one of the two auxiliary helium circulators stopped to reduce thermal stresses of the core graphite components, and thus helium flow rates of the auxiliary helium circulator decreased to about 0.78 and about 0.87 kg/s at the simulation tests from 15 and 30 MW operations, respectively. On the contrary, all the time after the startup of the auxiliary cooling system, water flow rate was fixed at about 20.0 kg/s by operating the two water pumps.

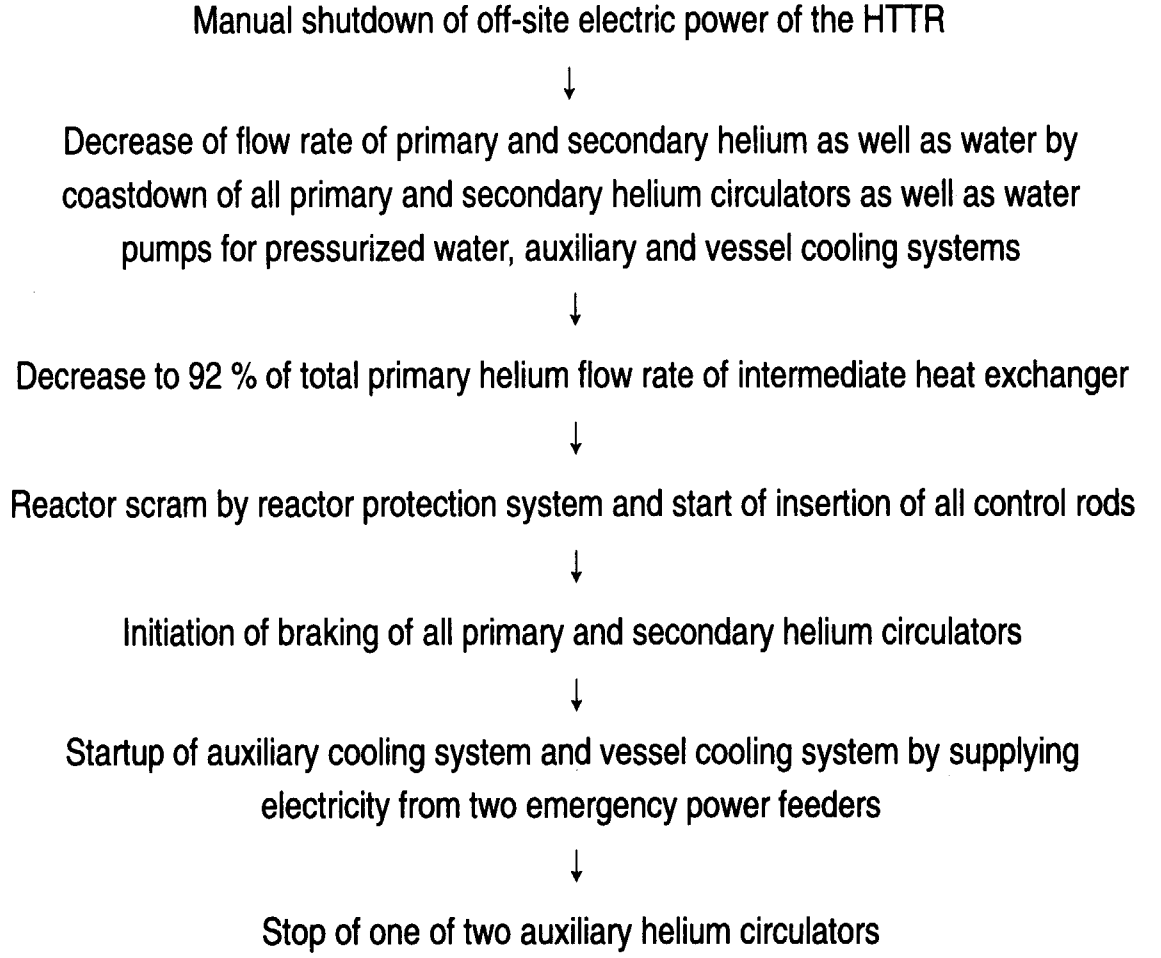

Fig. 3.1 Sequence of dynamic components during loss of off-site electric power simulation test from 15 MW operation

Manual shutdown of off-site electric power of the HTTR

↓

Decrease of flow rate of primary and secondary helium as well as water by coastdown of all primary and secondary helium circulators as well as water pumps for pressurized water, auxiliary and vessel cooling systems

↓

Decrease to 93 % of total helium flow rate of primary pressurized water cooler

↓

Reactor scram by reactor protection system and start of insertion of outer nine pairs of control rods

↓

Initiation of braking of all primary and secondary helium circulators

↓

Startup of auxiliary cooling system and vessel cooling system by supplying electricity from two emergency power feeders

↓

Start of insertion of inner seven pairs of control rods

↓

Stop of one of two auxiliary helium circulators

Fig. 3.2 Sequence of dynamic components during loss of off-site electric power simulation test from 30 MW operation

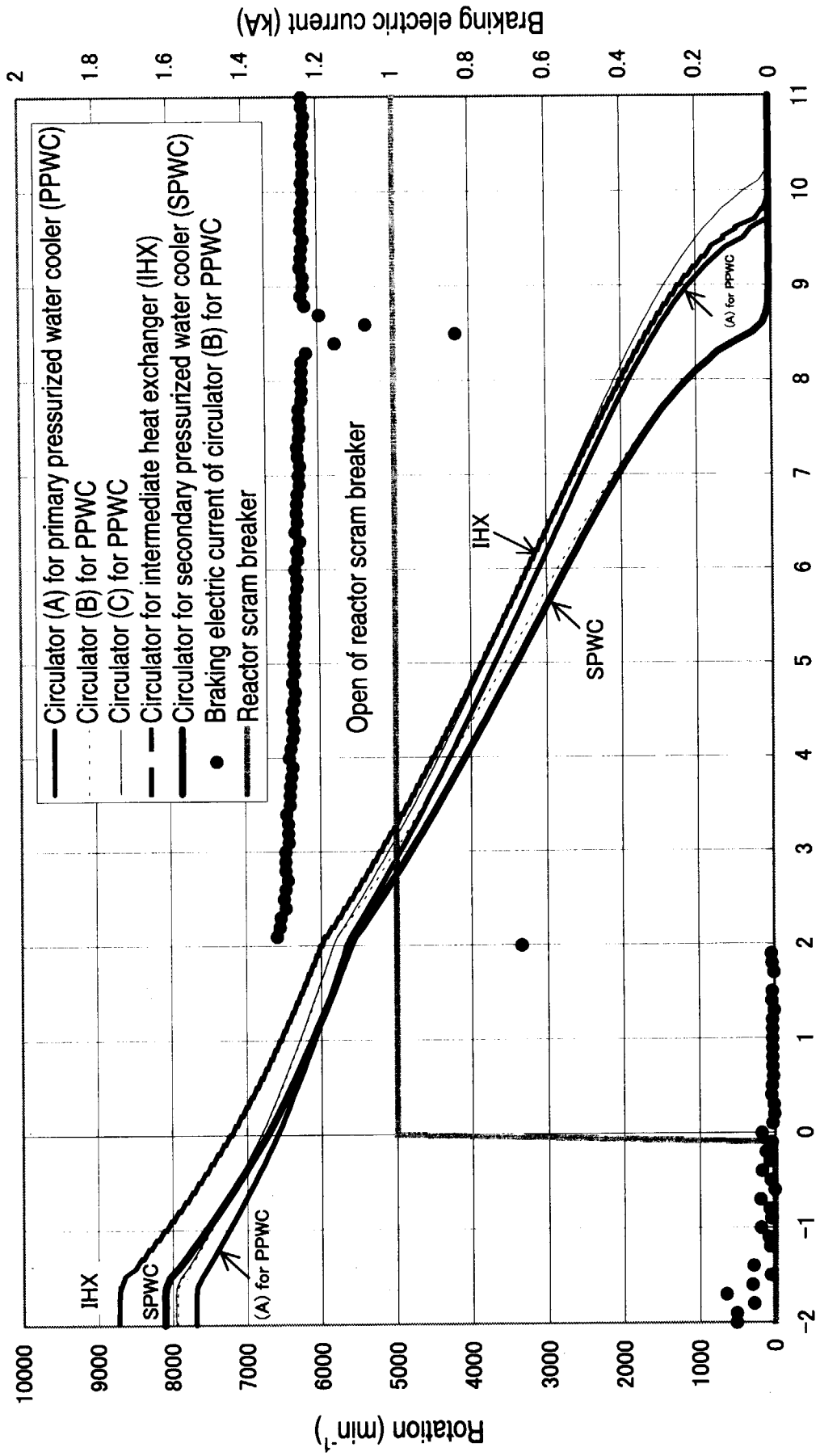

Fig. 3.3 Transient behaviors of rotations of all primary and secondary helium circulators during loss of off-site electric power simulation test from 15 MW operation

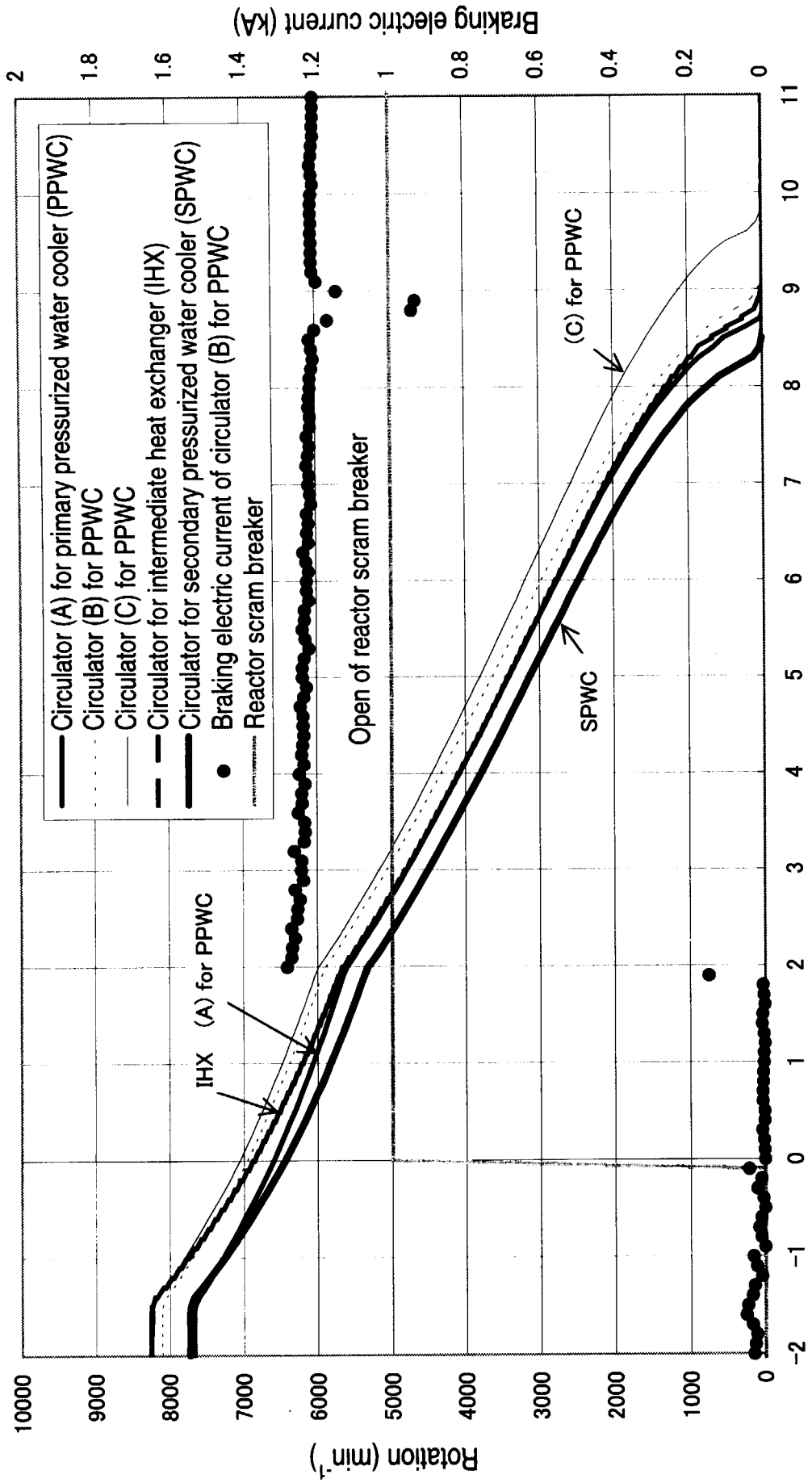

Fig. 3.4 Transient behaviors of rotations of all primary and secondary helium circulators during loss of off-site electric power simulation test from 30 MW operation

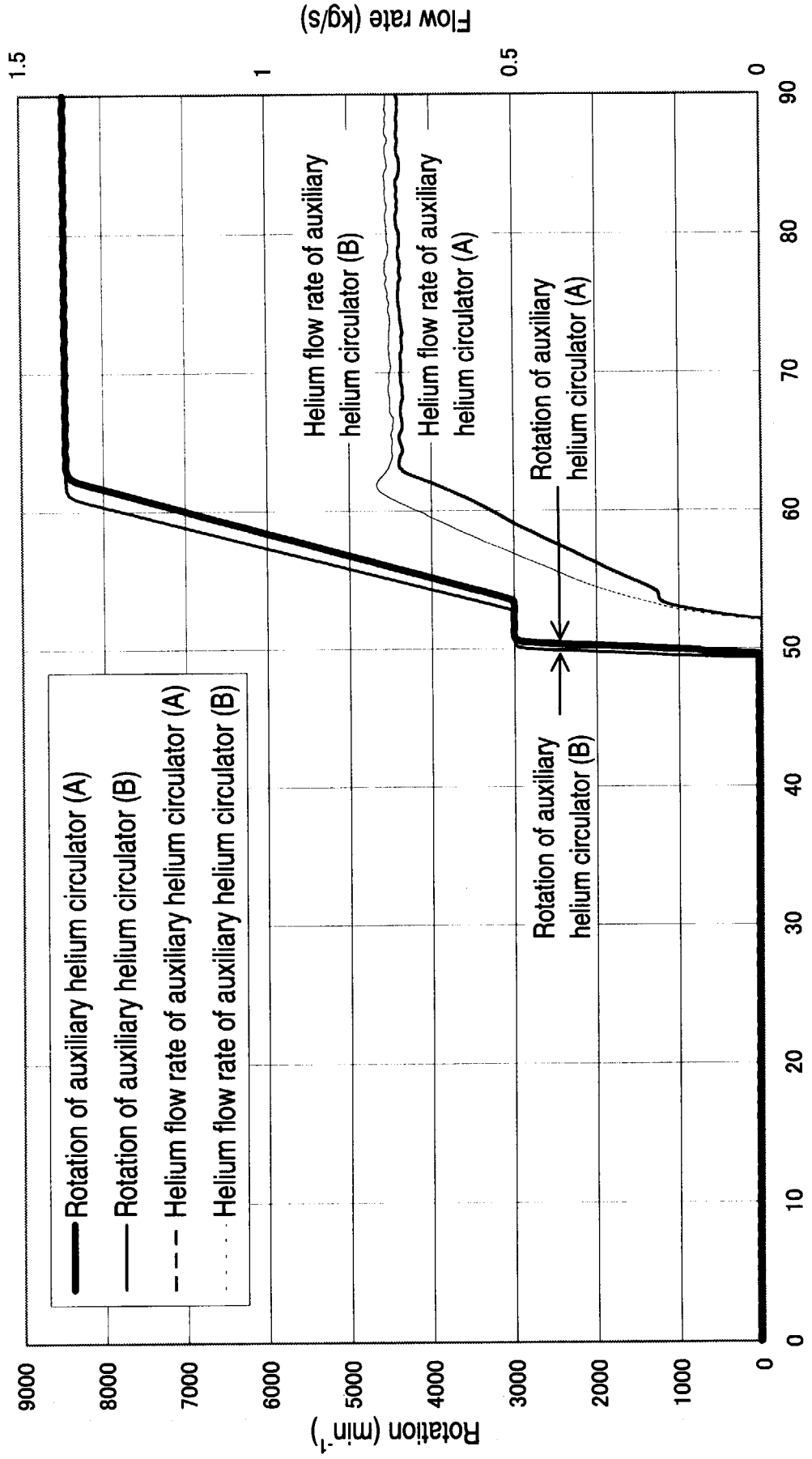

Fig. 3.5 Transient behaviors of rotation and flow rate of auxiliary helium circulators during loss of off-site electric power simulation test from 15 MW operation

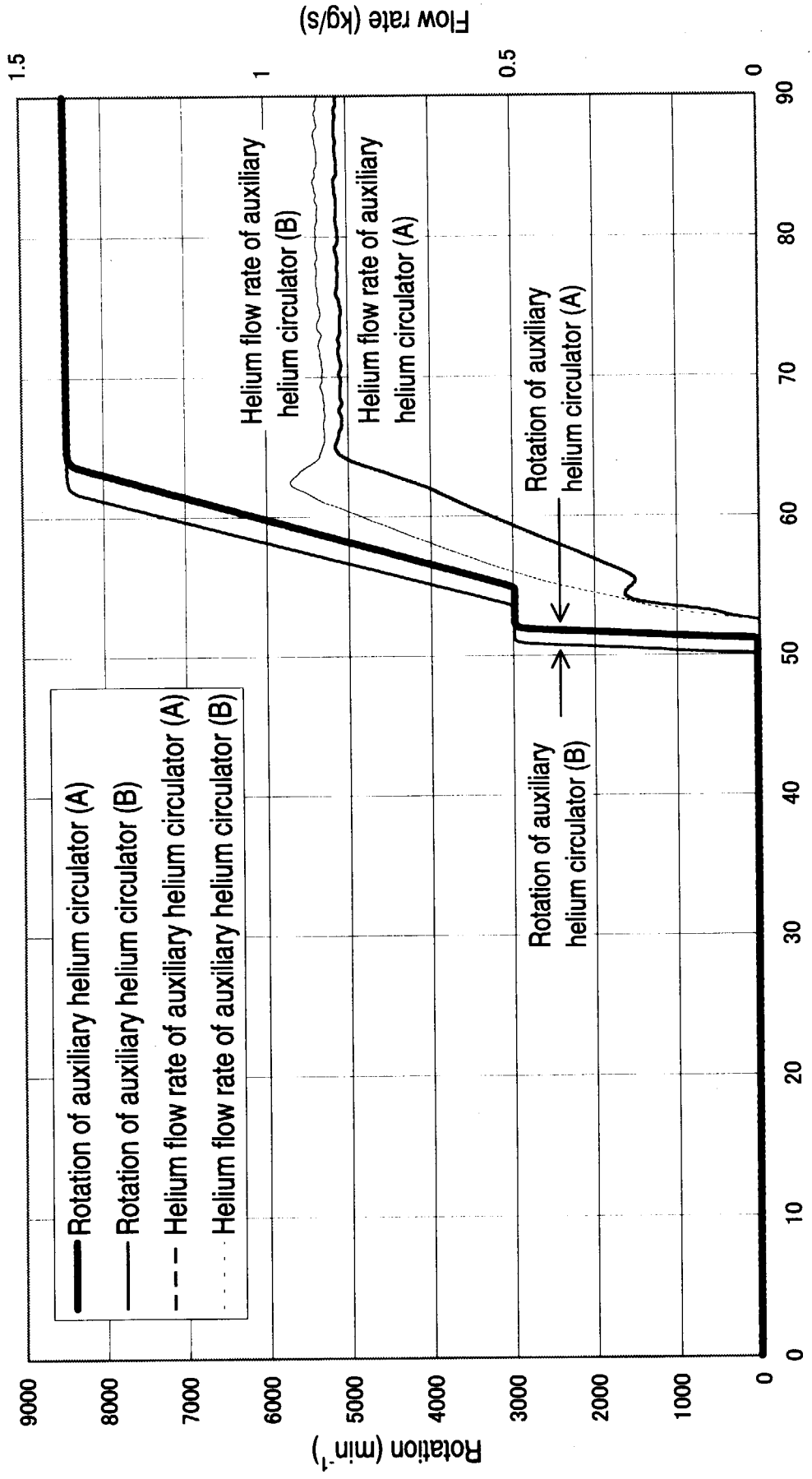

Fig. 3.6 Transient behaviors of rotation and flow rate of auxiliary helium circulators during loss of off-site electric power simulation test from 30MW operation

4. Behaviors of Reactor and its Cooling System at Simulation Tests

4.1 Conditions of Reactor and its Cooling System before Simulation Tests

Conditions of the reactor and its cooling system before the simulation tests are presented below. The simulation tests from 15 and 30 MW operations are designated as HTTR-LP(15MW) and HTTR-LP(30MW), respectively. Table 4.1 shows the thermal power, the reactor inlet and outlet coolant temperatures, the primary coolant pressure and flow rate as well as the hot plenum block temperature before the simulation tests. Figure 4.1 shows a cross-sectional view of the graphite blocks just below the active reactor core. Helium flows into the central penetration hole of the hot plenum block. Temperatures of helium flow into seven hot plenum blocks are measured in each block. Temperature of helium flow into the center hot plenum block was higher than those into the circumferential hot plenum blocks. Helium temperatures at the center and the circumferential hot plenum blocks were 478°C and about 470°C respectively before the simulation test from 15 MW operation, while 853°C and about 832°C before the simulation test from 30 MW operation. Temperatures of the hot plenum blocks are measured at representative three points. Because no significant temperature difference among the hot plenum blocks appeared, mean temperature among the hot plenum blocks was used for comparing with analytical results.

Tables 4.2, 4.3, 4.4 and 4.5 show the temperature, pressure and flow rate of the intermediate heat exchanger, the primary and secondary pressurized water coolers as well as the air cooler for the pressurized water cooling system before the simulation tests, respectively. The differential pressure between the primary helium and pressurized water as well as that between the primary and secondary helium were kept at the fixed values by the controlling systems. Tables 4.6 and 4.7 show the temperature, pressure and flow rate of the auxiliary heat exchanger and the air cooler for the auxiliary cooling system before the simulation tests, respectively. The auxiliary cooling system is in standby during the reactor normal operation. During the standby, the two auxiliary helium circulators were

not operated, however, a small amount of helium of 0.031 kg/s from the primary helium purification system was provided into the auxiliary cooling system to keep the auxiliary heat exchanger from thermal shock at the startup of the auxiliary cooling system. Furthermore, water pressure of the auxiliary cooling system was regulated through its controlling system, and one of the two water pumps for the auxiliary cooling system was driven. The water flow rate in standby was fixed at 5.6 kg/s.

Pressure ratio of outlet to inlet and invariant power of the helium circulators are denoted as functions of invariant rotation and invariant flow rate based on similarity law for fluid machinery. Temperature rise by the helium circulator is evaluated using a relationship among an invariant power, invariant flow rate and invariant rotation. Power is estimated by multiplying helium flow rate, specific heat of helium, difference between helium temperatures at inlet and outlet of the helium circulator. Invariant rotation (N'), invariant flow rate (G') and invariant power (Q') are calculated respectively from

$$N' = N / \sqrt{T_i} \quad (1)$$

$$G' = G \cdot \sqrt{T_i} / P_i \quad (2)$$

$$Q' = Q / (P_i \cdot \sqrt{T_i}) \quad (3)$$

where N is the rotation (min^{-1}), T_i is the helium inlet temperature (K), P_i is the helium inlet pressure (kg/cm^2 abs), G is the helium flow rate (kg/s), and Q is the power (W).

Figures 4.2 and 4.3 show design performance curves of the helium circulators for the primary and secondary helium cooling systems and the auxiliary cooling system, respectively [6]. Table 4.8 shows the pressure ratio of outlet to inlet and the invariant power of the primary and secondary helium circulators before the simulation tests. Table 4.9 shows the typical pressure ratio of outlet to inlet of the auxiliary helium circulators during the simulation tests.

4.2 Transient Behaviors of Reactor and its Cooling System during Simulation Tests

Transient behaviors of the reactor and its cooling system during the simulation tests are described below. Figures 4.4 and 4.5 show transient behaviors of the temperatures of the hot plenum block, the reactor inlet and outlet coolant during the simulation tests from 15 and 30 MW operations, respectively. The hot plenum block temperature decreased continuously after the startup of the auxiliary cooling system. The reactor inlet coolant temperature reduced rapidly by the startup of the auxiliary cooling system about 50 s later from the loss of off-site electric power. The reactor inlet coolant temperature decreased suddenly by the stop of one of the two auxiliary helium circulators 40 min later from the startup of the auxiliary cooling system, and since then it dropped gradually. The reactor outlet coolant temperature reduced continuously due to the insertion of the control rods and the startup of the auxiliary cooling system.

Figures 4.6 and 4.7 show transient behaviors of the primary coolant pressure and the reactor power during the simulation tests from 15 and 30 MW operations, respectively. The primary coolant pressure decreased gradually with reduction of the coolant temperature. The reactor power dropped drastically by the insertion of the control rods, and then the subcriticality of the reactor was maintained.

Figures 4.8 and 4.9 show transient behaviors of the heat removal of the auxiliary heat exchanger during the simulation tests from 15 and 30 MW operations, respectively. About 50 s later from the loss of off-site electric power the auxiliary cooling system started up, and subsequently about 10 min later flow rates and temperatures of helium and water became steady. Then the heat removal of the auxiliary heat exchanger was approximately 1.8 MW at the simulation test from 15 MW operation, while it was approximately 4.0 MW at the simulation test from 30 MW operation. The heat removal decreased suddenly by the stop of one of the two auxiliary helium circulators 40 min later from the startup of the auxiliary cooling system, and since then it dropped gradually.

Table 4.1 Conditions of reactor before simulation tests

Items	HTTR-LP(15MW)	HTTR-LP(30MW)
Thermal power	15MW	30MW
Reactor inlet coolant temperature	242°C	392°C
Reactor outlet coolant temperature	468°C	828°C
Primary coolant pressure	2.9MPa(abs)	4.0MPa(abs)
Primary coolant flow rate	12.4kg/s	12.4kg/s
Hot plenum block temperature	391°C	677°C

Table 4.2 Conditions of intermediate heat exchanger before simulation tests

Items	HTTR-LP(15MW)	HTTR-LP(30MW)
Primary helium inlet temperature	468°C	828°C
Primary helium outlet temperature	235°C	383°C
Primary helium pressure	2.8MPa(abs)	4.0MPa(abs)
Primary helium flow rate	4.1kg/s	4.1kg/s
Secondary helium inlet temperature	158°C	248°C
Secondary helium outlet temperature	420°C	751°C
Secondary helium pressure	2.9MPa(abs)	4.0MPa(abs)
Secondary helium flow rate	3.6kg/s	3.6kg/s

Table 4.3 Conditions of primary pressurized water cooler before simulation tests

Items	HTTR-LP(15MW)	HTTR-LP(30MW)
Helium inlet temperature	468°C	828°C
Helium outlet temperature	235°C	390°C
Helium pressure	2.8MPa(abs)	4.0MPa(abs)
Helium flow rate	8.2kg/s	8.2kg/s
Water inlet temperature	79°C	120°C
Water outlet temperature	100°C	160°C
Water pressure	2.3MPa(abs)	3.5MPa(abs)
Water flow rate	111kg/s	113kg/s

Table 4.4 Conditions of secondary pressurized water cooler before simulation tests

Items	HTTR-LP(15MW)	HTTR-LP(30MW)
Helium inlet temperature	420°C	751°C
Helium outlet temperature	152°C	243°C
Helium pressure	2.9MPa(abs)	4.0MPa(abs)
Helium flow rate	3.6kg/s	3.6kg/s
Water inlet temperature	79°C	120°C
Water outlet temperature	100°C	158°C
Water pressure	2.3MPa(abs)	3.5MPa(abs)
Water flow rate	57kg/s	59kg/s

Table 4.5 Conditions of air cooler for pressurized water cooling system before simulation tests

Items	HTTR-LP(15MW)	HTTR-LP(30MW)
Water inlet temperature	100°C	160°C
Water outlet temperature	45°C	66°C
Water pressure	2.2MPa(abs)	3.3MPa(abs)
Water flow rate	65kg/s	76kg/s
Air inlet temperature	7°C	8°C
Air outlet temperature	62°C	88°C
Air pressure	0.1MPa(abs)	0.1MPa(abs)
Air flow rate	270kg/s	370kg/s

Table 4.6 Conditions of auxiliary heat exchanger before simulation tests

Items	HTTR-LP(15MW)	HTTR-LP(30MW)
Helium inlet temperature	426°C	754°C
Helium outlet temperature	74°C	97°C
Helium pressure	2.8MPa(abs)	4.0MPa(abs)
Helium flow rate	0.031kg/s	0.031kg/s
Water inlet temperature	59°C	63°C
Water outlet temperature	62°C	71°C
Water pressure	1.3MPa(abs)	2.3MPa(abs)
Water flow rate	5.6kg/s	5.6kg/s

Table 4.7 Conditions of air cooler for auxiliary cooling system before simulation tests

Items	HTTR-LP(15MW)	HTTR-LP(30MW)
Water inlet temperature	62°C	71°C
Water outlet temperature	59°C	63°C
Water pressure	0.5MPa(abs)	1.5MPa(abs)
Water flow rate	5.6kg/s	5.7kg/s
Air inlet temperature	7°C	8°C
Air outlet temperature	8°C	9°C
Air pressure	0.1MPa(abs)	0.1MPa(abs)
Air flow rate	41kg/s	118kg/s

Table 4.8 Pressure ratio of outlet to inlet and invariant power of primary and secondary helium circulators before simulation tests

Items	HTTR-LP(15MW)			HTTR-LP(30MW)		
Helium circulator	PPWC	IHX	SPWC	PPWC	IHX	SPWC
Flow rate	2.7kg/s	4.1kg/s	3.6kg/s	2.7kg/s	4.1kg/s	3.6kg/s
Inlet temperature	234°C	235°C	153°C	385°C	383°C	243°C
Inlet pressure (abs)	2.8MPa	2.8MPa	2.9MPa	4.0MPa	4.0MPa	4.0MPa
Invariant flow rate	7760	11700	9010	6220	9320	7070
Rotation	8000min^{-1}	8770min^{-1}	8130min^{-1}	8160min^{-1}	8320min^{-1}	7760min^{-1}
Invariant rotation	355	389	394	318	325	341
Pressure ratio	1.0165	1.0159	1.0203	1.0138	1.0114	1.0159
Power	61	194	64	34	220	101
Invariant power	0.0938	0.3004	0.1049	0.0326	0.2099	0.1080

PPWC: Circulator (B) for primary pressurized water cooler, IHX: Circulator for intermediate heat exchanger, SPWC: Circulator for secondary pressurized water cooler

Table 4.9 Typical pressure ratio of outlet to inlet of auxiliary helium circulators during simulation tests

Items	HTTR-LP(15MW)				
Helium circulator	Auxiliary helium circulator (A)			Auxiliary helium circulator (B)	
Flow rate	0.72kg/s	0.66kg/s	0.79kg/s	0.75kg/s	0.68kg/s
Inlet temperature	128°C	183°C	146°C	130°C	180°C
Inlet pressure (abs)	2.8MPa	2.8MPa	2.7MPa	2.8MPa	2.8MPa
Invariant flow rate	1850	1800	2080	1920	1860
Rotation	8480min^{-1}	8480min^{-1}	8480min^{-1}	8480min^{-1}	8480min^{-1}
Invariant rotation	423	397	414	422	398
Pressure ratio	1.0066	1.0060	1.0055	1.0067	1.0061
Items	HTTR-LP(30MW)				
Helium circulator	Auxiliary helium circulator (A)			Auxiliary helium circulator (B)	
Flow rate	0.78kg/s	0.73kg/s	0.90kg/s	0.82kg/s	0.75kg/s
Inlet temperature	270°C	282°C	224°C	264°C	277°C
Inlet pressure (abs)	3.9MPa	3.8MPa	3.8MPa	3.9MPa	3.9MPa
Invariant flow rate	1650	1560	1860	1720	1620
Rotation	8480min^{-1}	8480min^{-1}	8470min^{-1}	8460min^{-1}	8460min^{-1}
Invariant rotation	364	360	380	365	361
Pressure ratio	1.0053	1.0050	1.0047	1.0053	1.0050

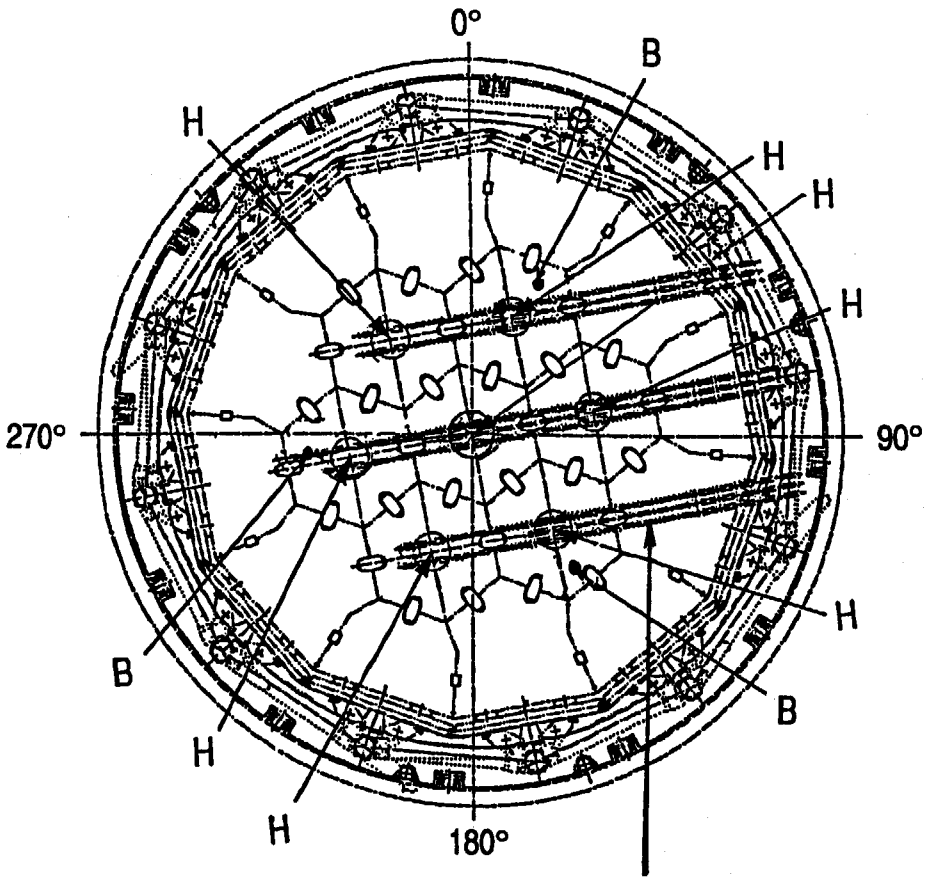

B; temperature of hot plenum block
H; temperature of helium flowing into hot plenum block

Fig. 4.1 Cross-sectional view of graphite blocks just below active reactor core

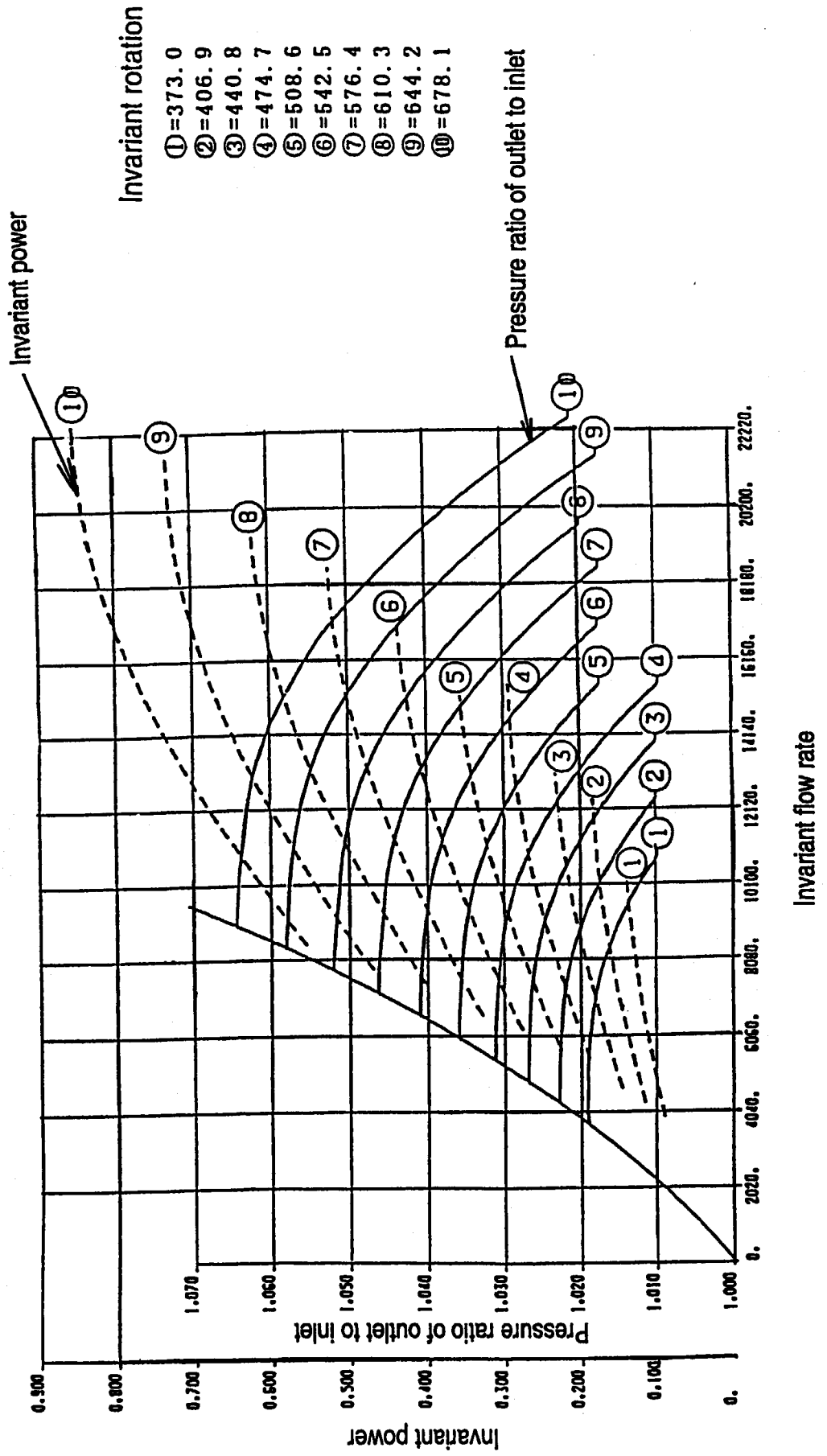

Fig. 4.2 Design performance curve of helium circulators for primary and secondary helium cooling systems

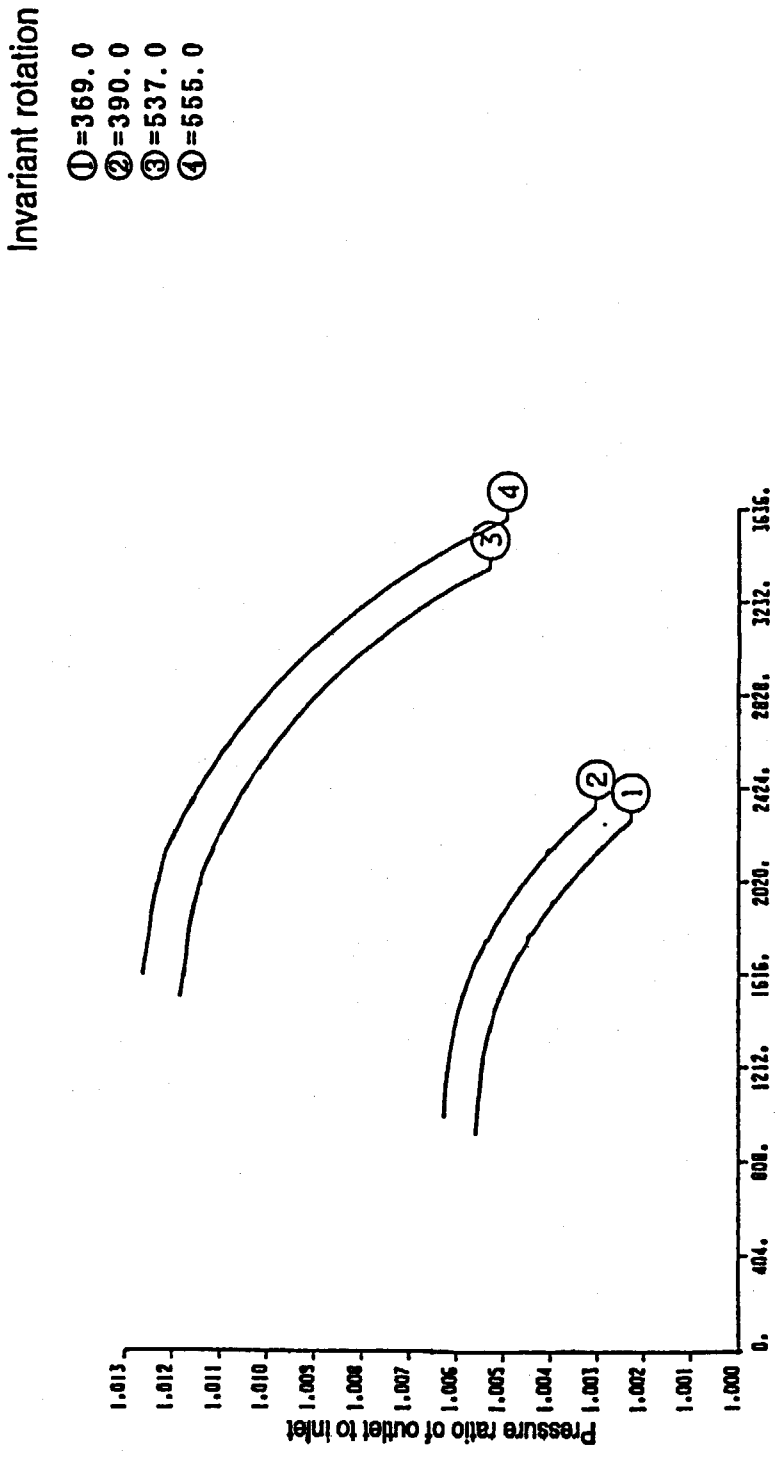

Fig. 4.3 Design performance curve of helium circulators for auxiliary cooling system

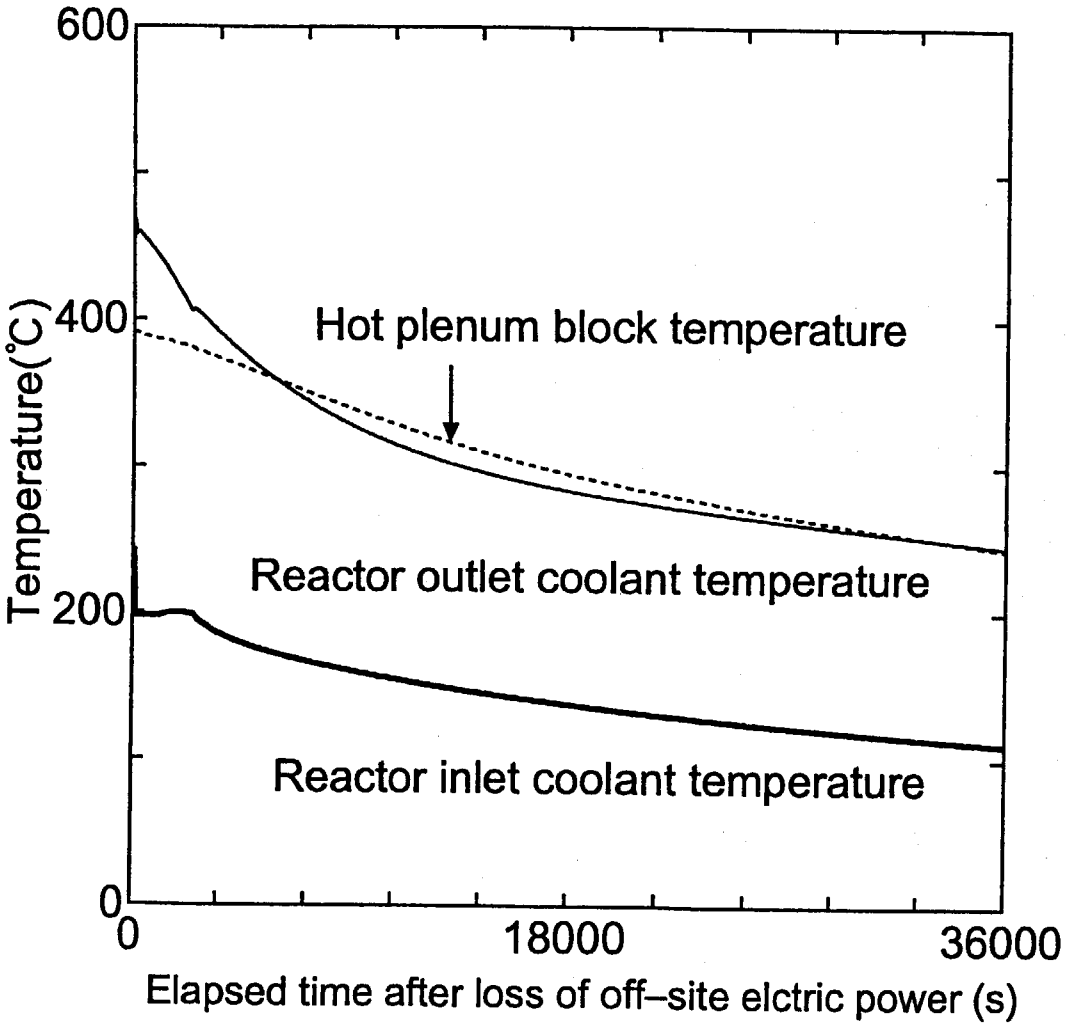

Fig. 4.4 Transient behaviors of temperatures of hot plenum block, reactor inlet and outlet coolant during loss of off-site electric power simulation test from 15 MW operation

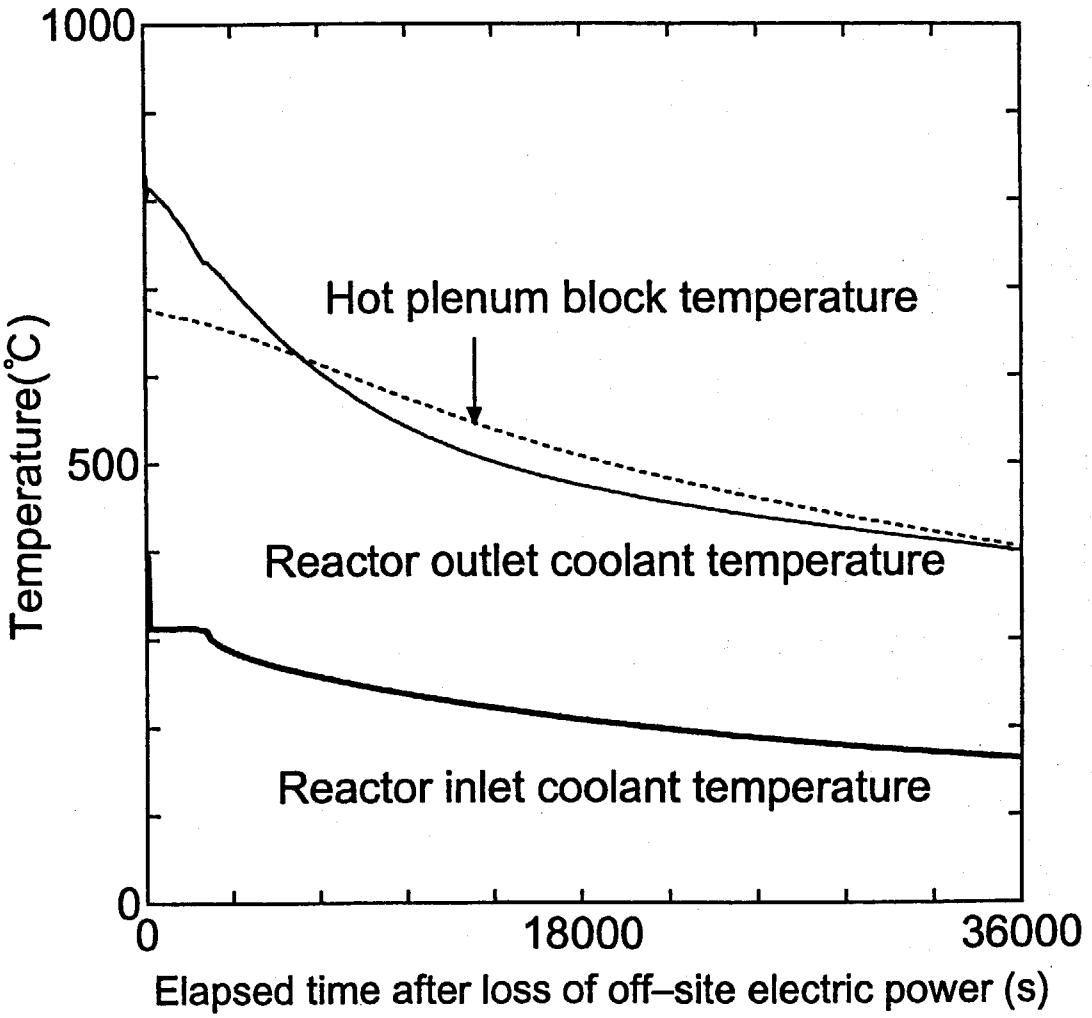

Fig. 4.5 Transient behaviors of temperatures of hot plenum block, reactor inlet and outlet coolant during loss of off-site electric power simulation test from 30 MW operation

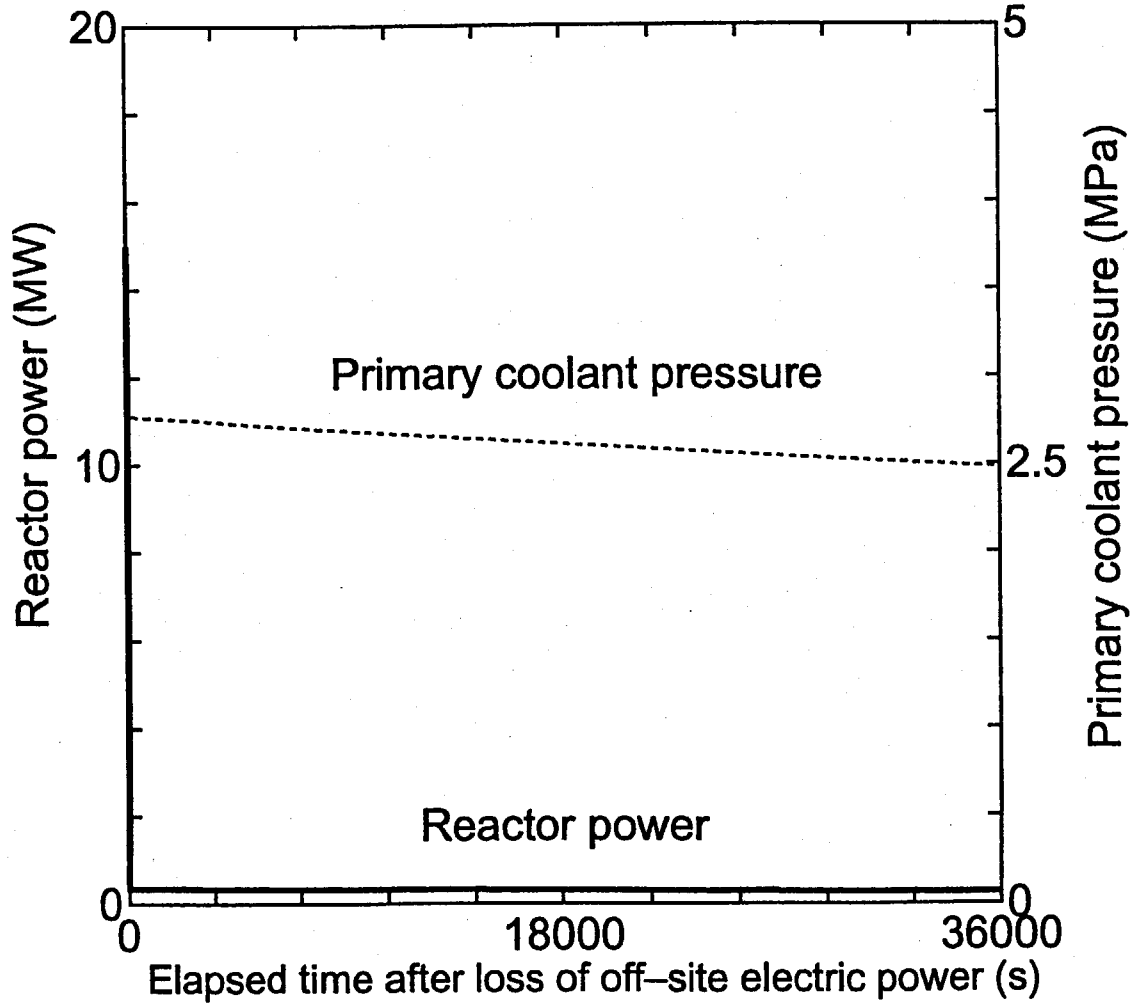

Fig. 4.6 Transient behaviors of primary coolant pressure and reactor power during loss of off-site electric power simulation test from 15 MW operation

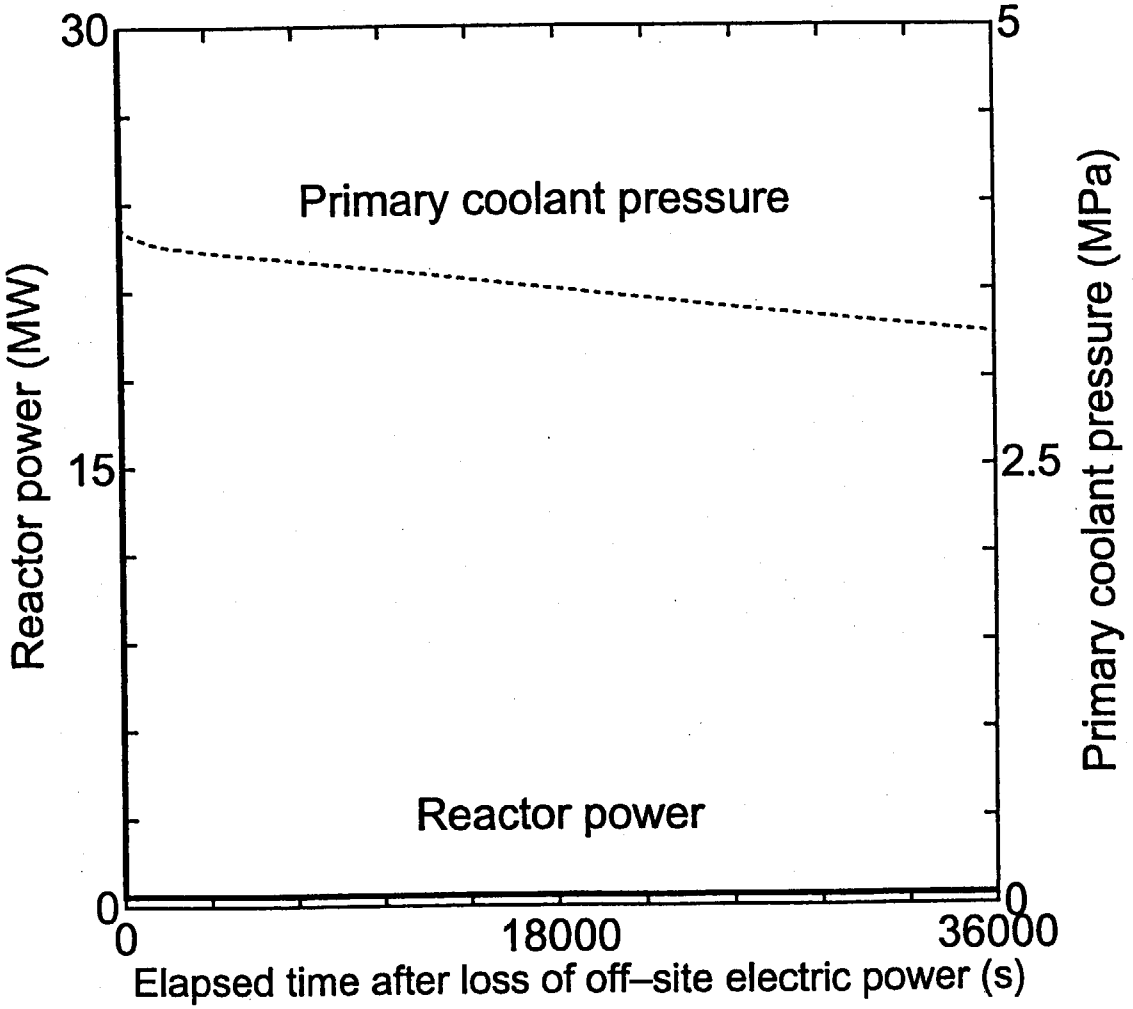

Fig. 4.7 Transient behaviors of primary coolant pressure and reactor power during loss of off-site electric power simulation test from 30 MW operation

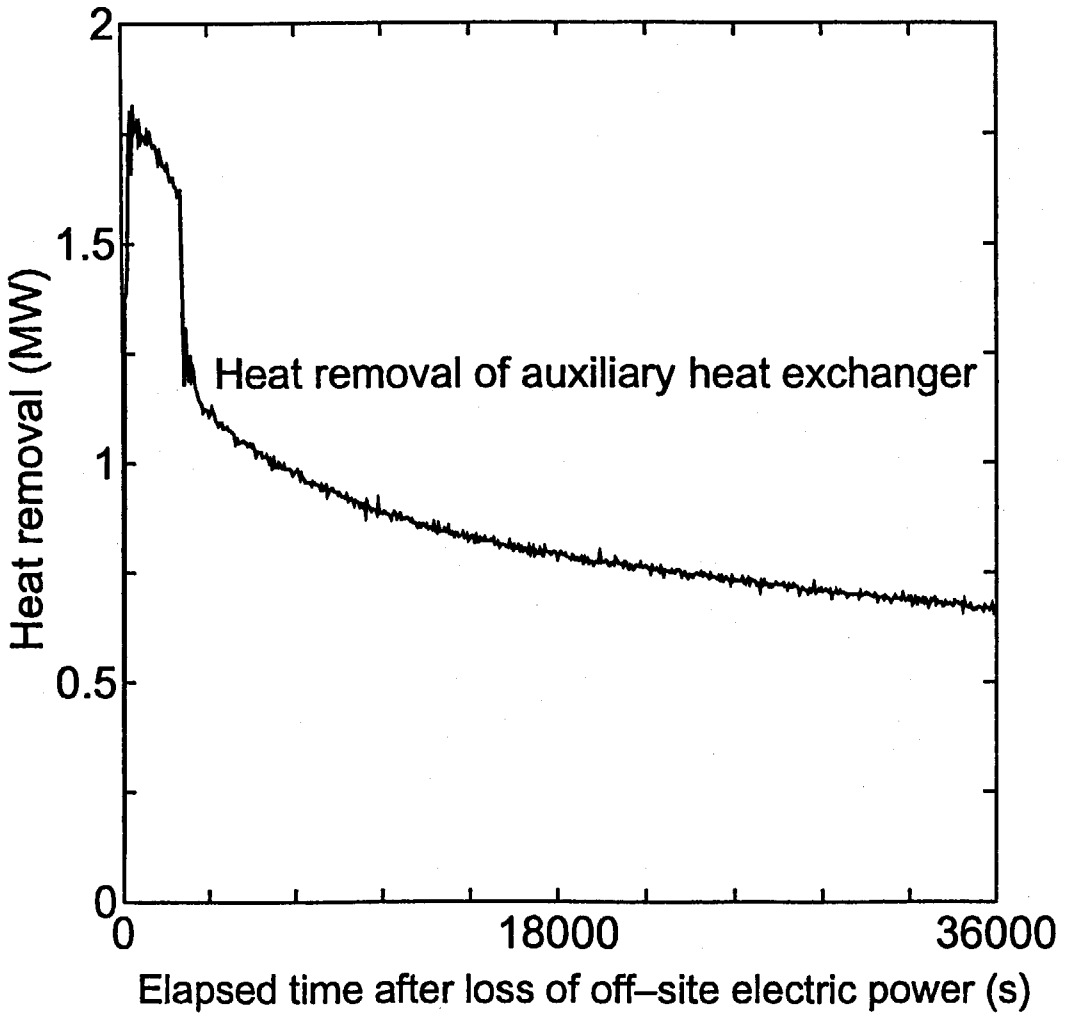

Fig. 4.8 Transient behavior of heat removal of auxiliary heat exchanger during loss of off-site electric power simulation test from 15 MW operation

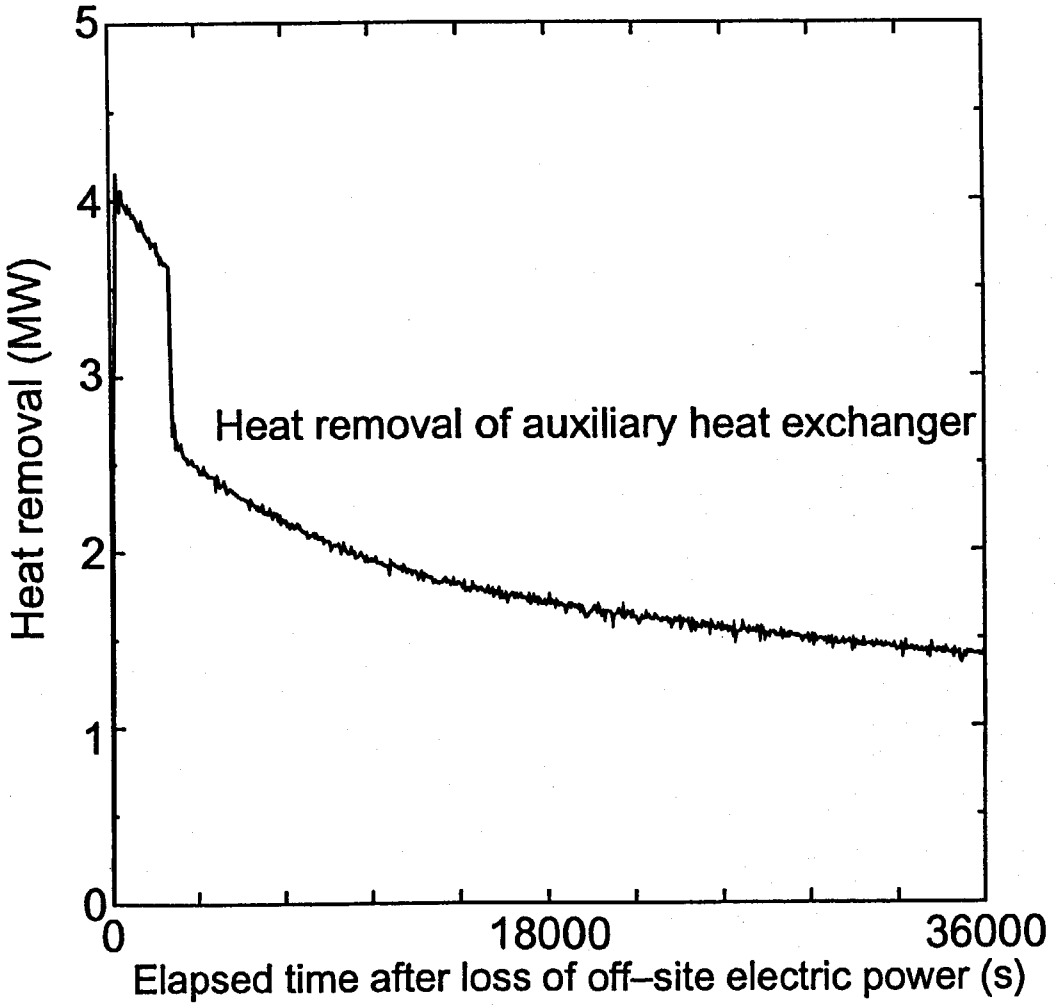

Fig. 4.9 Transient behavior of heat removal of auxiliary heat exchanger during loss of off-site electric power simulation test from 30 MW operation

5. Conclusions

In the rise-to-power test of the HTTR, simulation tests on loss of off-site electric power from 15 and 30 MW operations were conducted on March 1 in 2001 and on March 6 in 2002, respectively. Through the simulation tests, valuable data were obtained to validate analytical codes for plant dynamics of the HTGR such as 'ACCORD' code [7]. The followings are the major results from the simulation tests.

(1) Because helium circulators and water pumps coasted down immediately after the loss of off-site electric power, flow rates of helium and water decreased to the scram points. About 50 s later from the loss of off-site electric power, the auxiliary cooling system and the vessel cooling system started up by supplying electricity from two emergency power feeders.

(2) At the simulation test from 15 MW operation, all the control rods were inserted simultaneously into the reactor core by gravity. At the simulation test from 30 MW operation, the outer nine pairs of the control rods were inserted into the replaceable reflector region of the core at first, and 40 min later the other inner seven pairs fell into the fuel region. The reactor power dropped drastically by the insertion of the control rods, and then the subcriticality of the reactor was kept.

(3) About 10 min later from the startup of the auxiliary cooling system, flow rates and temperatures of helium and water of the auxiliary heat exchanger became steady. Then the heat removal of the auxiliary heat exchanger was approximately 1.8 MW at the simulation test from 15 MW operation, while it was approximately 4.0 MW at the simulation test from 30 MW operation. 40 min later from the startup of the auxiliary cooling system, one of two auxiliary helium circulators stopped. Temperature of hot plenum block decreased continuously after the startup of the auxiliary cooling system.

Sequences of the HTTR dynamic components were in accordance with the design. The information in this paper will be helpful in performing future high temperature test operation of the HTTR and in upgrading main components of the HTGR.

Acknowledgements

The authors would like to thank to the members of the department of HTTR project of Japan Atomic Energy Research Institute (JAERI). The authors also would like to thank to Drs K. Kunitomi and Y. Inagaki of JAERI for their useful comments.

References

(1) Saito, S., et al., Design of High Temperature Engineering Test Reactor, Report JAERI 1332, Japan Atomic Energy Research Institute, 1994.

(2) Takeda, T., Kunitomi, K., Ohkubo, M., Saito, T., Air Vent in Water Chamber and Surface Coating on Liner Slides concerning Auxiliary Cooling System for the High Temperature Engineering Test Reactor, Nucl. Eng. Des. 185, 229-240, 1998.

(3) Kunitomi, K., Nakagawa, S., Shinozaki, M., Passive Heat Removal by Vessel Cooling System of the HTTR during No Forced Cooling Accidents, Nucl. Eng. Des. 166, 179-190, 1996.

(4) Tachibana, Y., Shiozawa, S., Fukakura, J., Matsumoto, F., Araki, T., Integrity Assessment of the High Temperature Engineering Test Reactor (HTTR) Control Rod at Very High Temperature, Nucl. Eng. Des. 172, 93-102, 1997.

(5) Takeda, T., Nakagawa, S., Tachibana, Y., Takada, E., Kunitomi, K., Analytical Evaluation on Loss of Off-site Electric Power Simulation of the High Temperature Engineering Test Reactor, Report JAERI-Research 2000-016, Japan Atomic Energy Research Institute, 2000.

(6) GEC ALSTHOM (RATEAU), private communication.

(7) Takeda, T., Tachibana, Y., Kunitomi, K., Itakura, H., Development of Analytical Code 'ACCORD' for Incore and Plant Dynamics of High Temperature Gas-cooled Reactor, Report JAERI-Data/Code 96-032, Japan Atomic Energy Research Institute, 1996 (in Japanese).

This is a blank page.

国際単位系（SI）と換算表

表1　SI基本単位および補助単位

量	名称	記号
長さ	メートル	m
質量	キログラム	kg
時間	秒	s
電流	アンペア	A
熱力学温度	ケルビン	K
物質量	モル	mol
光度	カンデラ	cd
平面角	ラジアン	rad
立体角	ステラジアン	sr

表2　SIと併用される単位

名称	記号
分，時，日	min，h，d
度，分，秒	°，′，″
リットル	l，L
トン	t
電子ボルト	eV
原子質量単位	u

1 eV=1.60218×10^{-19}J

1 u=1.66054×10^{-27}kg

表3　固有の名称をもつSI組立単位

量	名称	記号	他のSI単位による表現
周波数	ヘルツ	Hz	s^{-1}
力	ニュートン	N	m·kg/s^2
圧力，応力	パスカル	Pa	N/m^2
エネルギー,仕事,熱量	ジュール	J	N·m
工率，放射束	ワット	W	J/s
電気量，電荷	クーロン	C	A·s
電位，電圧，起電力	ボルト	V	W/A
静電容量	ファラド	F	C/V
電気抵抗	オーム	Ω	V/A
コンダクタンス	ジーメンス	S	A/V
磁束	ウェーバ	Wb	V·s
磁束密度	テスラ	T	Wb/m^2
インダクタンス	ヘンリー	H	Wb/A
セルシウス温度	セルシウス度	℃	
光束	ルーメン	lm	cd·sr
照度	ルクス	lx	lm/m^2
放射能	ベクレル	Bq	s^{-1}
吸収線量	グレイ	Gy	J/kg
線量等量	シーベルト	Sv	J/kg

表4　SIと共に暫定的に維持される単位

名称	記号
オングストローム	Å
バーン	b
バール	bar
ガル	Gal
キュリー	Ci
レントゲン	R
ラド	rad
レム	rem

1 Å=0.1nm=10^{-10}m

1 b=100fm^2=10^{-28}m^2

1 bar=0.1MPa=10^{5}Pa

1 Gal=1cm/s^2=10^{-2}m/s^2

1 Ci=3.7×10^{10}Bq

1 R=2.58×10^{-4}C/kg

1 rad=1cGy=10^{-2}Gy

1 rem=1cSv=10^{-2}Sv

表5　SI接頭語

倍数	接頭語	記号
10^{18}	エクサ	E
10^{15}	ペタ	P
10^{12}	テラ	T
10^9	ギガ	G
10^6	メガ	M
10^3	キロ	k
10^2	ヘクト	h
10^1	デカ	da
10^{-1}	デシ	d
10^{-2}	センチ	c
10^{-3}	ミリ	m
10^{-6}	マイクロ	μ
10^{-9}	ナノ	n
10^{-12}	ピコ	p
10^{-15}	フェムト	f
10^{-18}	アト	a

（注）

1．表1－5は「国際単位系」第5版，国際度量衡局1985年刊行による。ただし,1 eVおよび1 uの値はCODATAの1986年推奨値によった。

2．表4には海里，ノット，アール，ヘクタールも含まれているが日常の単位なのでここでは省略した。

3．barは，JISでは流体の圧力を表わす場合に限り表2のカテゴリーに分類されている。

4．EC閣僚理事会指令ではbar，barnおよび「血圧の単位」mmHgを表2のカテゴリーに入れている。

換算表

力	N(=10^{5}dyn)	kgf	lbf
	1	0.101972	0.224809
	9.80665	1	2.20462
	4.44822	0.453592	1

粘度　1 Pa·s(N·s/m^2)=10 P(ポアズ)(g/(cm·s))

動粘度　1m^2/s=10^{4}St(ストークス)(cm^2/s)

圧力	MPa(=10bar)	kgf/cm^2	atm	mmHg(Torr)	lbf/in^2(psi)
	1	10.1972	9.86923	7.50062×10^3	145.038
	0.0980665	1	0.967841	735.559	14.2233
	0.101325	1.03323	1	760	14.6959
	1.33322×10^{-4}	1.35951×10^{-3}	1.31579×10^{-3}	1	1.93368×10^{-2}
	6.89476×10^{-3}	7.03070×10^{-2}	6.80460×10^{-2}	51.7149	1

エネルギー・仕事・熱量	J(=10^7 erg)	kgf·m	kW·h	cal(計量法)	Btu	ft·lbf	eV
	1	0.101972	2.77778×10^{-7}	0.238889	9.47813×10^{-4}	0.737562	6.24150×10^{18}
	9.80665	1	2.72407×10^{-6}	2.34270	9.29487×10^{-3}	7.23301	6.12082×10^{19}
	3.6×10^6	3.67098×10^5	1	8.59999×10^5	3412.13	2.65522×10^6	2.24694×10^{25}
	4.18605	0.426858	1.16279×10^{-6}	1	3.96759×10^{-3}	3.08747	2.61272×10^{19}
	1055.06	107.586	2.93072×10^{-4}	252.042	1	778.172	6.58515×10^{21}
	1.35582	0.138255	3.76616×10^{-7}	0.323890	1.28506×10^{-3}	1	8.46233×10^{18}
	1.60218×10^{-19}	1.63377×10^{-20}	4.45050×10^{-26}	3.82743×10^{-20}	1.51857×10^{-22}	1.18171×10^{-19}	1

1 cal= 4.18605J（計量法）

= 4.184J（熱化学）

= 4.1855J（15℃）

= 4.1868J（国際蒸気表）

仕事率　1 PS(仏馬力)

= 75 kgf·m/s

= 735.499W

放射能	Bq	Ci
	1	2.70270×10^{-11}
	3.7×10^{10}	1

吸収線量	Gy	rad
	1	100
	0.01	1

照射線量	C/kg	R
	1	3876
	2.58×10^{-4}	1

線量当量	Sv	rem
	1	100
	0.01	1

（86年12月26日現在）

Data on Loss of Off-site Electric Power Simulation Tests of the High Temperature Engineering Test Reactor